The
ENGINEERS' DIGEST

REVIEW OF ENGINEERING PROGRESS ABROAD

VOL. V. No. 4 APRIL, 1944

CHURCHILL CENTRELESS GRINDING MACHINES.
Built for precision work and continuous high production.

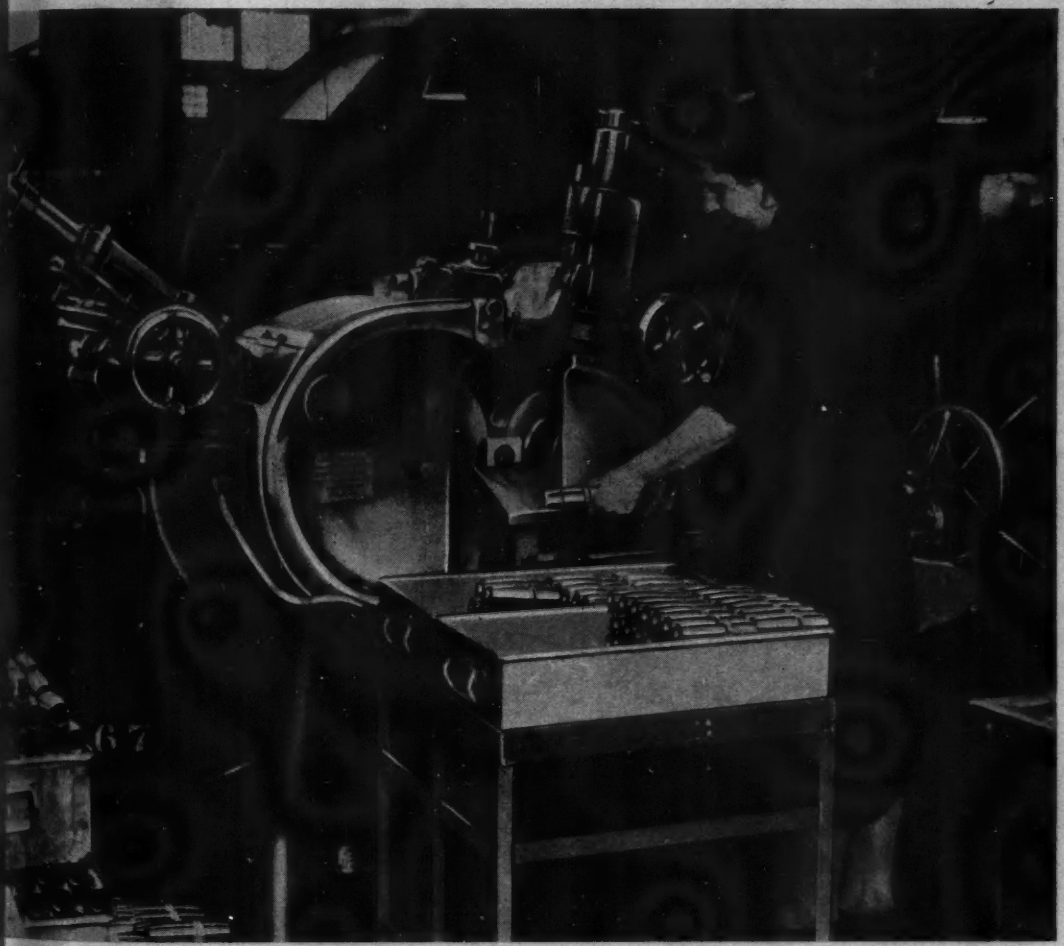

THE CHURCHILL MACHINE TOOL CO. LTD., BROADHEATH, Nr. MANCHESTER

THE ENGINEERS' DIGEST

REVIEW OF ENGINEERING PROGRESS ABROAD

Published Monthly at 120, Wigmore Street, London, W. 1.

Publishers : **ENGINEERS' DIGEST LTD.** – – – – Telephone : WELBECK 9357

Advertisement Dept. – 120, Wigmore Street, London, W.1 – Telephone : Welbeck 9357

Distribution – – E. & F. N. SPON, LTD., 57, Haymarket, London, S.W.1
Telephone : Whitehall 1860. Telegrams : Fenspon, Lesquare, London

Editorial Dept. – – 120, Wigmore Street, London, W.1. – Telephone : Welbeck 9357

Subscriptions to : ENGINEERS' DIGEST LTD., 120, Wigmore Street, London, W.1, or
E. & F. N. SPON, LTD., 57, Haymarket, London, S.W.1

ANNUAL SUBSCRIPTION OF 12 NUMBERS, £2 2s. SINGLE COPIES, 4s. 6d.

ADVISORY COMMITTEE

J. F. ALCOCK, B.A., A.M.I.Mech.E.
R. W. ALLOTT, M.A., A.R.Ae.S.
E. ALTON, D.Eng., A.M.Inst.B.E.
H. H. ASBRIDGE, M.B.E., M.I.Mech.E.
R. W. AYERS, M.I.W.
Col. J. BOWDEN, M.Inst.C.E., M.I.Mech.E.
H. H. BROUGHTON, M.I.Mech.E.
F. BUCKINGHAM, B.Sc., A.M.Inst.C.E., A.M.I.Mech.E.,
T. H. BURNHAM, B.Sc. (Lond.), A.M.I.Mech.E. [A.M.I.E.E.
J. S. CASWELL, M.Sc., M.I.Mech.E.
G. C. SAFFERY COOPER.
J. DICK, Ph.D., B.Sc., A.M.I.Mech.E.
D. FIFE, M.I.Mech.E.
G. E. FOXWELL, D.Sc. (Lond.), F.Inst.P., F.Inst.F., M.Inst.
R. GRIFFITHS, M.Sc. [Gas.E.
H. HEYWOOD, Ph.D., M.Sc. (Eng.), A.M.I.Mech.E.
O. HURST, M.Inst.N.A.
Capt. J. S. IRVING, M.I.Mech.E., M.I.A.E., A.F.R.Ae.S., M.S.A.E.
F. C. JOHANSEN, M.Sc. (Eng.), M.I.Mech.E., F.R.Ae.S., M.I.Loco.E.
W. J. KEARTON, D.Eng., M.I.Mech.E., A.M.Inst.N.A.
Prof. W. KERR, Ph.D., M.I.Mech.E.
G. V. LOMONOSOFF, Dr.Ing., M.I.Mech.E.
B. J. LYMER, M.I.Mech.E.
D. T. MacIVOR, M.I.Mech.E., M.Cons.E.
W. O. MANNING, F.R.Ae.S.
R. B. MATTHEWS, Wh.Ex., A.M.Inst.C.E., M.I.E.E., F.R.Ae.S.
Prof. A. L. MELLANBY, D.Sc., LL.D., M.I.Mech.E.
J. H. R. RATCLIFFE, B.Sc. (Eng., Hons.), M.I.Mech.E.
Col. C. W. D. ROWE.
W. A. SCOBLE, D.Sc., A.R.C.Sc., M.I.Mech.E.
P. W. SEEWER, D.E. (Zurich), M.Inst.C.E., M.I.Mech.E.
Prof. S. PARKER SMITH, D.Sc., M.I.E.E., A.M.Inst.C.E.
C. E. H. VERITY, A.M.Inst.C.E., A.M.I.E.E., A.M.I.Mech.E.
E. G. WALKER, F.C.G.I., B.Sc. (Eng.), M.Inst.C.E., M.I.Mech.E., M.Am.Soc.C.E.
Major F. L. WATSON, M.Inst.C.E., M.I.Mech.E.
G. WATSON, M.Inst.C.E., M.I.Mech.E.
C. H. WOODFIELD, M.I.Mech.E., M.I.Struct.E.
T. WRIGHT, Ph.D., M.Sc.
M. L. YATES, Ph.D., M.Sc.Tech., M.A. (Com.), M.I.Mech.E.

A "SABEN"
HIGH SPEED STEEL
10% SABEN TUNGSTEN
14% SABEN TUNGSTEN
18% SABEN EXTRA TUNGSTEN
22% SABEN KERAU TUNGSTEN
6% SABEN WUNDA COBALT
10% SABEN TENCO COBALT
FOR EVERY NEED
A low Tungsten Steel for Hot Die work. Special feature.—To withstand High Temperatures without cracking.
A good reliable High Speed Steel for Taps, Drills, Boring and Turning Tools, Punches, etc.
The Standard 18-4-1 High Speed Steel for all Metal Cutting Tools, Twist Drills, Milling Cutters, etc.
A Steel with just that extra bit of quality to tackle those special jobs that make hard going for lower Tungsten Brands.
For Machining Nickel Chrome Steels, High Manganese Steels and Castings.
For the toughest of all Machining Jobs. Specially recommended where customers' machines are not adapted for the use of Carbide Tools.
Our Booklet B.6 gives full details of these Steels, and is available on request.
THESE ARE ALL STANDARD QUALITIES TRIED, TESTED AND PROVED. WAR-TIME GOVERNMENT RESTRICTIONS MAY HAVE CAUSED THE TEMPORARY SUBSTITUTION OF OTHER ANALYSES, BUT SOME ARE STILL AVAILABLE, AND OUR SERVICES AND ADVICE ARE AT CUSTOMERS' DISPOSAL.
SANDERSON BROTHERS & NEWBOULD LTD SHEFFIELD

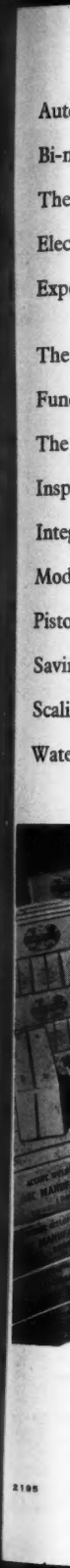

CONTENTS

	page
Automatic Mixer for Producer Gas Engines *"The Engineers' Digest," Vol. 5, No. 4, p. 120.*	120
Bi-metallic Pyrometer *"The Engineers' Digest," Vol. 5, No. 4, p. 104.*	104
The Effectiveness of the Airscrew as a Landing Brake *"The Engineers' Digest," Vol. 5, No. 4, p. 115.*	115
Electrical Energy Consumption in Electrolytical Processes *"The Engineers' Digest," Vol. 5, No. 4, p. 99.*	99
Experimental Determination of the Stress Concentration Factor due to an Abrupt Change in the Diameter of a Shaft in Torsion *"The Engineers' Digest," Vol. 5, No. 4, p. 98.*	98
The Extinction of the Arc in Single and Multiple Break Air Blast High Speed Circuit Breakers *"The Engineers' Digest," Vol. 5, No. 4, p. 108.*	108
Fundamental Equation of Mechanics of Flight *"The Engineers' Digest," Vol. 5, No. 4, p. 93.*	93
The Influence of Diameter upon the Properties of Steel Cable *"The Engineers' Digest," Vol. 5, No. 4, p. 111.*	111
Inspection of Sparking Plugs as a Means of Checking Engine Operation *"The Engineers' Digest," Vol. 5, No. 4, p. 105.*	105
Integrating Machine for Solving Ordinary Differential Equations *"The Engineers' Digest," Vol. 5, No. 4, p. 94.*	94
Modern Isolating Switches for Indoor Use *"The Engineers' Digest," Vol. 5, No. 4, p. 118.*	118
Piston Area as the Basis of Similarity Consideration *"The Engineers' Digest," Vol. 5, No. 4, p. 96.*	96
Saving and Substitution of Critical Material *"The Engineers' Digest," Vol. 5, No. 4, p. 113.*	113
Scaling of Locomotive Boilers *"The Engineers' Digest," Vol. 5, No. 4, p. 101.*	101
Water Circulation in Bent-tube and Radiant Boilers *"The Engineers' Digest," Vol. 5, No. 4, p. 109.*	109

TO GET THE BEST ELECTRODES

Specify **ACTARC**

and **SUREARC**

ACTARC SUREARC

REGD. TRADE MARK

ARC MANUFACTURING CO., LTD.

PROPRIETORS OF THE SURE-ARC ELECTRODE CO., LTD

ACTARC WORKS, GOLDHAWK ROAD, LONDON, W.12

TELEPHONE: SHE 1151 TELEGRAMS: ACTIVARC, PHONE, LONDON. CABLES: ACTIVARC, LONDON.

2185

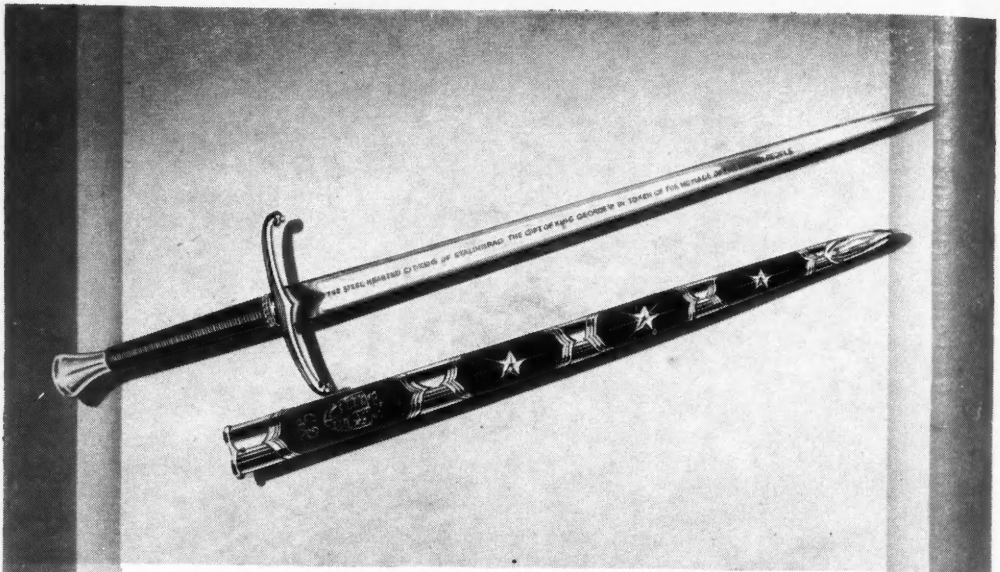

Craftsmanship

The Sword of Stalingrad. Not only a token of the homage paid by our people to the citizens of that immortal city, but an example of all that is best in British Craftsmanship. The same craftsmanship, together with modern methods of manufacture, is employed to produce Wimet Dies. The vital element of these dies is the Wimet insert with its unequalled resistance to abrasive materials. Wimet dies, due to the closely controlled processing and manufacture, have many outstanding advantages, such as increased accuracy, greater uniformity of carbide inserts, superior finish, to mention only a few, all of which make for increased production. They are available for Wire, Tube and Round Bar, Hexagon Bar or Square Bar Drawing. Special Presswork Dies are supplied to suit customers' needs.

A.C. Wickman LIMITED
• COVENTRY • ENGLAND •

LONDON BRISTOL BIRMINGHAM MANCHESTER LEEDS GLASGOW NEWCASTLE

FUNDAMENTAL EQUATION OF MECHANICS OF FLIGHT.

Reviewed by A. PRÖLL, *VDI.** (From *Zeitschrift des VDI*, Vol. 87, Nos. 23/24, June 12th, 1943, pp. 345-346).

THE extensive literature on mechanics of flight has been supplemented in a remarkable way by G. A. Crocco, whose new definitions simplify the subject and bring it into a clearer system.

DEFINITION OF INDUCTION.

The coefficient of induced drag is given as $c_w = c_{wo} + \frac{c_a^2}{A}$ (c_{wo} is the so-called residual drag coefficient, c_a the lift coefficient, $A = \frac{b^2}{F}$ the aspect ratio for span b and wing area F). Assuming aerodynamically clean design, Crocco puts $i = \frac{3}{4}$ as an average value, and points out that both performance and flight behaviour can be deduced from a few fundamental quantities.

The first of the quantities introduced by him is that of "Induction" (j) which is a characteristic value in all flight altitudes. (For ceiling it tends towards its maximum, j = 3). Under induction the ratio $\frac{BC}{AB}$ in the polar diagram (Fig. 1) is understood at the point C, which for a given power corresponds to the maximum speed v_o. The relationship between v_o and j is expressed by the following equation

$$v_o^4 = \frac{z}{j} \frac{i\, q_\delta}{A\, c_{wo}\, \rho_o^2} \quad .. \quad .. \quad .. \quad (1)$$

[z = altitude, q_δ = "relative wing loading" $= \frac{g}{F}\left(\frac{\rho}{\rho_o}\right)$; g = acceleration of gravity, ρ = density of air].

Another new definition is the "economic power ratio" H, which is the ratio of required power at minimum gliding angle to maximum available power.

It can be calculated to

$$H = 2\frac{j^{\frac{3}{2}}}{1+j} \quad .. \quad .. \quad (2)$$

Further $j = \left(\frac{v_E}{v_o}\right)^4$, where v_E is the speed at minimum gliding angle ϵ_{min}. In Fig. 2, j is plotted against altitude z with H_o as parameter. H_o is H at z=o). In this plot the differences between the various types of aircraft are clearly brought out.

EXAMPLE OF APPLICATION.

Consider for example a uniformly retarded horizontal turn. The initial speed (maximum speed) be v_o, the initial radius $R_o = \frac{v_o^2}{g\sqrt{n_o^2 - 1}}$. "Isogonal flight" is assumed where the angle of bank γ is constant, whereby the load factor increases from $n = n_u$ to n_o, while v decreases from v_o to v_u. Denoting the ratio $\frac{v}{v_o} = x$, φ the Azimuth angle, and s the distance covered at the time t, we have three integrals

$$\left.\begin{aligned} \varphi &= \frac{2}{\epsilon_{min}}\sqrt{j\,(n^2-1)}\int_1^x \frac{-x\,dx}{x^4-(1+j)\,x+n^2\,j} \\ t &= \frac{1}{g}\sqrt{\frac{2}{\rho_o}}\sqrt{\frac{q_\delta}{\epsilon_{min}\,c_{wo}}}\sqrt[4]{j}\int_1^x \frac{-x^2\,dx}{x^4-(1+j)\,x+n^2\,j} \\ s &= \frac{q_\delta}{g\,\rho_o\,c_{wo}}\int_1^x \frac{-x^2\,dx}{x^4-(1+j)\,x+n^2\,j} \end{aligned}\right\} \quad (3)$$

Crocco calculates a fighter with values as follows: $\epsilon_{min} = 1/12.5$, $c_{wo} = 0.0256$, A = 6, G/F = 128 kg/sq.m. (wing loading), the maximum speed at 4000 m. altitude is v_o = 138.5 m. sec. (500 km/hr.). Then, $q_\delta = 128\ \rho_o/\rho = 191$ kg/sq.m., j = 1/16 [from eq. (1)], H = 0.236 [from eq. (2)]. By use of formulae not reproduced here Crocco obtains the power loading G/N = 2.7 kg/h.p. With a load factor $n_o = 4$, for $\varphi = \pi$ (180°) we obtain x = 0.885. For this half turn s = 1481 m., covered in t = 11.3 seconds. The initial radius is R_o = 495 m. For a turn of uniform speed, the radius becomes R_u = 296 m. (dotted circle in Fig. 3). The load factor is here smaller, n_u = 2.867, so is the (constant) speed $v_u = 0.643\ v_o$.

CONCEPT OF MOST ECONOMIC ALTITUDE z_E.

Crocco introduces the concept of most economic altitude as the altitude at which the speed for minimum gliding angle is identical with the maximum obtainable speed (then $v_E/v_o = 1$, j = 1 and H = 1). For great speeds the value of z_E is very great too, e.g., for $v_o = v_E$ = 700 km. hr. z_E = 19.4 km. Of course, with the decrease of the speed of sound with altitude, the Mach

*The reviewer gives a cross-section of the 170-page book of G. Arturo Crocco, "Begriffsgleichungen der Flugmechanik," which has been published in Italian and German as Shriften der Deutsch. Akad. d. Luftfahrtforschung, No. 38, München and Berlin, 1941, by R. Oldenburg.

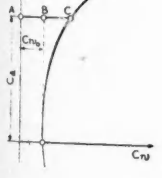

$j = \frac{BC}{AB}$

Fig. 1

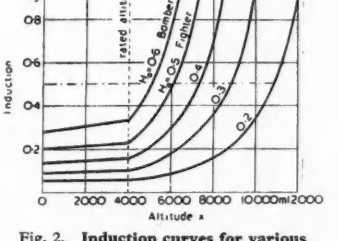

Fig. 2. **Induction curves for various altitudes.**

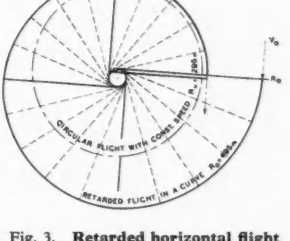

Fig. 3. **Retarded horizontal flight in curve.**

numbers increase, and the most economic altitude will be lower than that given by z_E.

SIMILARITY CONSIDERATIONS AND "ISONOMY."

A new term has been derived called "Isonomy" and Crocco defines it as the similarity between two aircraft that enables them to execute a given flight manoeuvre with the same time and with the same speed. In this case five parameters must be identical, i.e., c_{w_o}, A, i, $q\delta$ and the power loading G/N.

Isomony is fundamentally different from mechanical or geometrical similarity; its significance for aircraft is similar to that of Froude's law for ships.

INTEGRATING MACHINE FOR SOLVING ORDINARY DIFFERENTIAL EQUATIONS.

By PROF. DR. R. SAUER and DR. ING. H. POESCH, VDI. (From *Zeitschrift des VDI*, Vol. 87, Nos. 15/16, April 17th, 1943, pp. 221-224).

ORDINARY differential equations, or systems of such, occur in many technical investigations, particularly in those concerned with oscillations and with questions of stability. Very often the loss of time incurred in the solution of such problems and the number of personnel required to execute numerical or graphical solutions by methods of trial and error, etc., is quite intolerable. This applies in particular to cases where entire families of curves are to be established in order to ascertain the influence of certain parameters. A differential analyser for solving differential equations was built for the first time by V. Bush at Massachussetts Institute of Technology[1]. A substantially identical replica of this machine was built at Manchester by D. R. Hartree, and also by S. Rosseland[2] at Oslo; while several such machines are to be used in the Soviet Union. An up-to-date unit of this type was recently constructed in Germany, which unit is in successful operation.

Basic Principles and their Realisation.

In this new machine all variables t, x, etc., are represented by the angular rotation of shafts. The input "bus shaft" assigned to the independently variable t is driven by a motor at the desired speed in such a manner that the variation of the interdependent angular rotations corresponds to the differential equation to be solved. The result can either be given graphically by charting the curves $x = x(t)$, etc., or it can be given in numerical form by means of a printing device. Placing of a differential equation on the machine is effected by appropriate coupling of the bus shafts through integrators, input and output "tables," adders, and ratio-gears.

An integrator unit is shown in Fig. 1. Here, the rotation of the disc (a) is taken off by a lightweight, sharp-edged roller (b), so that the angular rotation (x) of the disc, and the distance (y) of the roller from the disc centre are in the functional inter-relationship $dx = C\,y\,dz$. By appropriate choice of scale, this expression can be made $dz = y\,dz$. With a given angular rotation (x) of the disc, effected by the input bus shaft, and with a given displacement of the roller in the direction of the y-axis, the output shaft receives the angular rotation

$$z = \int y\,dx.$$

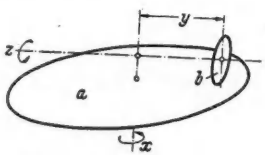

Fig. 1. **Principle of the integrator,**

$$z = \int y.dx.$$

(a) Disc (b) Roller

The underlying principle of the input table will be readily understood by referring to Fig. 2. Here the y-axis rotates the drum (c), around which is wrapped a sheet of paper or celluloid; while the carriage (d) is displaced by means of a lead screw along a spindle parallel with the axis of the drum. This input table, therefore, serves to "feed" a given function $y = y(x)$ into the machine. For this purpose a pointer on the carriage is made to follow the curve charted on the paper wrapped around the drum, while the drum is rotated by the drive. Movement of the pointer is effected by turning the carriage spindle by hand, or it can also be carried out automatically by means of a photoelectric cell, or with the use of a template. Conversely, this device is used as output table; in this case, both shafts are driven by the machine, and the output curve $y = y(x)$ is charted by a recording pen affixed to the carriage.

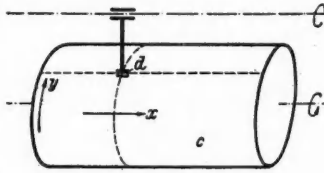

Fig. 2. **Principle of the functional drive (input or output table). $y = f(x)$.**

(c) Drum
(d) Carriage

The adders consist of differential gears in which the revolutions of a driven shaft are the sum or difference of the revolutions of two leading shafts. In the ratio drives, the revolutions of the shafts involved are in a ratio given by the ratio of a set of spur gears.

The four principal elements of the machine are schematically outlined in Figs. 3-6. Here the ± sign denotes that the input drives of the integrators, and both shafts of the input and output tables, as well as the input drives A and B of the adders can be made to operate in either rotational direction. The ratio drives can be coupled to the output shafts of the integrators, and to either shaft of the input and output tables, and also to the input shafts A and B of the adders. The initial distance (y) of the rollers of the integrators can be set by hand with an accuracy of plus or minus 10 microns.

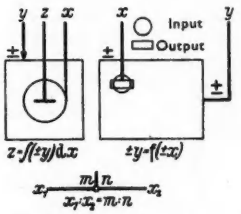

Figs. 3-6. **Schematical representation of the four basic components of the machine.**

$$x_r \frac{m/n}{x_1 x_2 + m \cdot n} x_2$$

The t—shaft is driven by an electric motor, while the rotation of the output shaft of each component element of the machine is electrically synchronised with the rotation of the input shaft of the driven component element. Since the friction of the rollers on their respective discs is too small to drive the component element

1 J. Franklin Inst., Vol. 212, 1931, p. 447.
2 Naturwiss., Vol. 27, 1939, p. 729; also ETZ, Vol. 61, 1940, p. 33.

coupled to the output shaft of the respective integrator, the output shafts are equipped with electric torque amplifiers. If this amplification becomes insufficient when a large number of component elements is coupled together, special torque amplifiers can be inserted wherever required. In order to enable adjustment of the machine to be made by mathematically unskilled personnel, a switch board will preferably be provided for the realisation of the set-ups required for the solution of the differential equations which can be handled by the machine.

Determination of the Required Set-up.

With the aforementioned four types of components, the machine can be set for the solution of all linear and of very general classes of non-linear ordinary differential equations of any order. Multipliers as additional component element may be useful in some cases, but they are not necessary in principle, as the products $u(x)\,v(y)$ of two functions, as well as the integrals $\int u(x)\,v(y)\,dz$ of such products can also be formed by means of two integrators respectively. The method followed in setting up the machine for a given differential equation may be exemplified by the case of an impressed oscillation with linear characteristics, and with a damping effect proportional with the speed.

In this case, the differential equation

$$\frac{d^2q}{dt^2} + b\frac{dq}{dt} + q = O$$

(b = constant) is fed into the machine in the form

$$\frac{dq}{dt} + bq + \int qdt = O.$$ According to Fig. 7, the machine is set up as follows: Integrator I to handle $q = \int \frac{dq}{dt}\,dt$, Integrator II to handle $bq = \int bdq$ with constant b, Integrator III to handle $\int q\,dt$, and adder S to deal with $\frac{dq}{dt} = -bq - \int qdt$

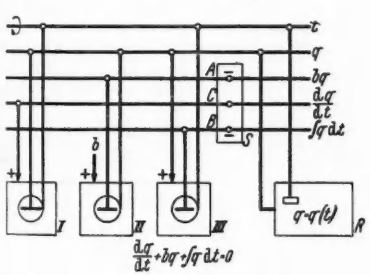

Fig. 7. **Set-up for the equation $\frac{dq}{dt} + b\frac{dq}{dt} + q = O$ (b = const).**

The output table R is coupled to the t and q shafts for drawing the curve $q = q(t)$. For rational values of b, the integrator II can be replaced by a ratio gear with m:n = b. In order to obtain a definite solution, the input sides of the integrators III and I must be set for initial values $q = q_o$ of the oscillator, and $\frac{dq}{dt} = \left[\frac{dq}{dt}\right]_o$ respectively before operation of the machine is commenced.

Accuracy of the Machine.

According to S. Rosseland, the accuracy of the machine can be ascertained by investigating the equation $\frac{d^2x}{dt^2} + x = O$, or $\frac{dx}{dt} + \int x\,dt = O$.

This requires the set-up shown in Fig. 8. In this case the two integrators yield

$$x = \int \frac{dx}{dt}\,dt \quad \text{and} \quad \frac{dx}{dt} = \int \frac{d^2x}{dt^2} = \int (-x)\,dt \quad \text{respectively}$$

With initial values of $x_o = r$, and $\left[\frac{dx}{dt}\right]_o = O$, it is found $x = r \cos t$, and $\frac{dx}{dt} = -r \sin t$. By coupling the output table R to the x and $\frac{dx}{dt}$ shafts, the final curve obtained as output will be given by $x^2 + \left(\frac{dx}{dx}\right)^2 = r^2$ which of course is a circle. With ten complete circles of $r = 175$ mm. described by the output table, an error of abt. 0.5mm. was found, which is equivalent to an error of abt. 0.05 mm. per complete revolution, or 0.03 per cent.

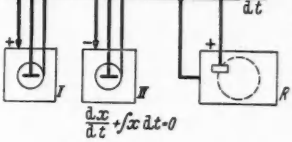

Fig. 8. **Set-up for ascertaining the accuracy of the machine.**

NON-ELEMENTARY OSCILLATION PROBLEMS.

Even with no more than two integrators and one input and one output table, integration problems can be solved which have no solution by means of elementary methods.

Free Oscillation with Non-linear Characteristic.

While in the ordinary oscillator the constraining force f is proportional with the amplitude q, in the case of " pseudoharmonic " oscillators, this force is given by the non-linear function $f = f(q)$. The non-linear differential equation

$$\frac{d^2q}{dt^2} + f(q) = O \text{ or } \frac{dq}{dt} + \int f(q)\,dt = O$$

generally does not admit of a ready solution. However, its integration by the machine is nearly as simple as that of the elementary case. According to Fig. 9, this is accomplished with the use of two integrators I and II to

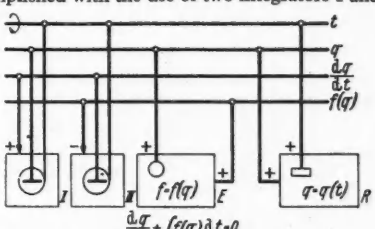

Fig. 9. **Set-up for the equation $\frac{dq}{dt} + \int f(q)\,dt = O$.**

give $q = \int \frac{dq}{dt}\,dt$ and $\frac{dq}{dt} = \int [-f(q)]\,dt$, and also with the use of the input table E for feeding in the function $f = f(q)$.

Free Oscillations with the Constraining Force varying with Time.

With the so-called "rheolinear" oscillator, the constraining force f is in proportionality with the amplitude, but this proportionality factor also varies with the time in a given functionality. Again, no ready solution exists for the differential equation $\frac{d^2q}{dt^2} + q\,f(t) = O$ or $\frac{dq}{dt} + \int q\,f(t)\,dt = O$, but this can easily be integrated by resorting to the set-up shown

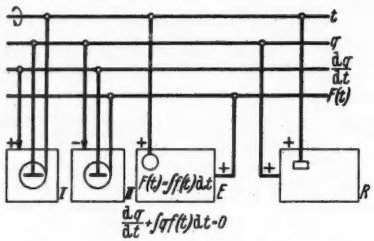

Fig. 10. **Set-up for the equation $\frac{dq}{dt} + q\,f(t) = O$.**

in Fig. 10. Here the two integrators I and II yield

$$q = \int \frac{dq}{dt}\,dt \text{ and } \frac{dq}{dt} = \int (-q)\,dF.$$

while the input table E gives $F = f(t)\,dt$.

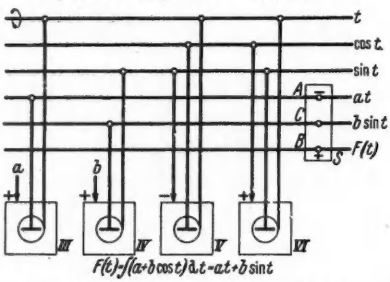

Fig. 11. **Set-up in combination with set-up Fig. 10 for solving Mathieu's equation.**

Of great practical and theoretical importance is the special case of Mathieu's differential equation with $f(t) = a + b \cos t$, that is $F = a\,t + b \sin t$. For this case, the integrator E is replaced by the arrangement shown in Fig. 11, so that according to Figs. 10 and 11 a set-up is obtained which comprises six integrators I to VI, one adder S, and the output table R. The input sides of the integrators III and IV are set for constant a and b values. Under certain conditions, the integrators III and IV can be replaced by ratio-gears.

Harmonic Analysis and Differentiation.

The machine can also be used for establishing the Fourier coefficients

$$\int_0^{2\pi} f(t)\,d(\cos nt) \text{ and } \int_0^{2\pi} f(t)\,d(\sin nt).$$

This is effected by using two integrators for the formation of cos nt and sin nt respectively, while another integrator is employed for the integrals of f(t).

According to H. Bueckner[3], differentiation of a given function f(t) can be carried out with the employment of the set-up shown in Fig. 12. It can be easily shown that for a sufficiently large value of n, the differential equation

$$\frac{1}{n}\frac{dy}{dt} + y = \frac{df(t)}{dt}, \text{ or } \frac{1}{n}y + \int y\,dt = f(t)$$

can be replaced by the approximation $y = \frac{dt}{d} \cdot f\left(t - \frac{1}{n}\right)$.

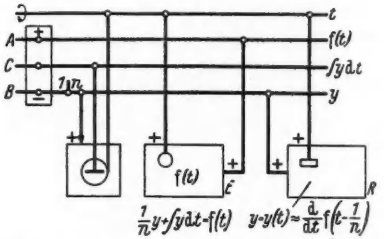

Fig. 12. **Set-up for differentiation according to H. Bueckner.**

In the set-up given in Fig. 12, the function f(t) to be differentiated is fed into the machine at the input table E. By adjusting the integrator to an initial value of $y_o = \frac{d}{dt} f\left(1 - \frac{1}{n}\right)$ of the differential quotient, the output table R connected to the bus shafts t and y, will then yield the approximate differential curve. In cases where the function f(t) is a straight line or is parabolic, the differential curve will even be strictly accurate. Although there are certain inaccuracies involved in the execution of the differentiation process by the machine, results obtained so far are said to be satisfactory.

3 Z. Angew. Math. Mech., Vol. 22, 1942, p. 143.

PISTON AREA AS THE BASIS OF SIMILARITY CONSIDERATION.

By P. RIEKERT, Automotive Research Institute of the Technical College, Stuttgart. (From *Luftfahrtforschung*, Vol. 20, No. 4, April 30th, 1943, pp. 99-101).

THE POWER OF THE SINGLE CYLINDER ENGINE.

THE power in a single cylinder can be found from the mean effective pressure p_{me} [kg./cm.²], the piston area F [m.²], the stroke s [m], and the engine speed n [min.⁻¹] by the relation

$$N_e = \frac{10^4\,p_{me}\,F\,s\,n}{2\times 60\times 75} = \frac{p_{me}\,F\,s\,n}{0.9} \text{ [h.p.]} \quad .. (1)$$

Introducing the capacity $V_h = Fs \times 10^3$ [1], the specific volumetric power is obtained

$$\frac{Ne}{V_h} = \frac{p_{me}\,n}{900} \text{ [h.p./l]} \quad .. \quad .. \quad (2)$$

For multi-cylinder engines it is more useful to express $\frac{Ne}{F}$, the power per piston area in terms of the mean

piston speed $c_m = \frac{s\,n}{30}$ [m./sec.]. Thus from eq. (1)

$$\frac{Ne}{F} = \frac{p_{me}\,c_m}{300} \text{ [h.p./cm.}^2\text{]} \quad .. \quad .. \quad (3)$$

The mean pressure of the ideal engine (index v) can be estimated by equating the work done during one stroke with the work due to transformation of the energy of fuel. Thus, $p_{mv}\ Fs = p_{mv}\ V_h\ 10$ [*mkg.*]. For the complete combustion of fuel a certain minimum amount of air is required, and so a certain amount of fuel can be burnt in the unit volume—the so-called calorific value of the mixture, H_u/V_g (kcal./m.^{3}). In this, H_u (kcal/kg.) is the lower calorific value per unit weight, and V_g (m.^{3}/kg.) the minimum volume of mixture required per kg. of fuel.

The summing up for a single cylinder of capacity V_h (1) gives

$$p_{mv}\ V_h \times 10 = 427 \eta_v \frac{H_u}{V_g} V_h \times 10^{-3}, \text{ or}$$

$$p_{mv} = 427\ \eta_v \frac{H_u}{V_g}\ 10^{-4} \text{ (kg./cm.}^2\text{)} \quad .. \quad (4)$$

For self-suction engines with $\frac{H_u}{V_g} = 900$ kcal./m.^{3} and the efficiency $\eta_v = 0.5$ the mean pressure becomes $p_{mv} = 19.2$ kg./cm.^{2}. The practical value p_{me} is, owing to thermal and other losses, lower than p_{mv}. As the mean pressure is independent of the dimensions of the engine it represents a true index value. An increase of the mean pressure is possible by supercharging, i.e., an increase in H_u/V_g. A decrease in the cylinder dimensions results in shorter paths of thermal conductance in the piston and a lower temperature of the piston head. Therefore, with decreasing cylinder dimensions the mean pressure can be increased.

A second index value is the mean piston speed c_m. It characterizes also the bearing loads in geometrically similar cylinders. Denoting with m (kg./m.$^{-1}$ s^2) the moving masses; $r = \frac{s}{2}$ (m) the crank radius; $\omega = \frac{\pi n}{30}$ (s^{-1}) the angular velocity, and f (cm.^{2}) the bearing area, the bearing pressure k due to acceleration forces, can be expressed as

$$k = \frac{m\,r\,\omega^2}{f} = \frac{\pi^2}{60} \frac{m\,c_m\,n}{f} \text{ (kg./cm.}^2\text{)} \quad .. \quad (5)$$

For geometrically similar design the masses are proportional to the third powers and the bending areas to the squares of the linear dimensions. From eq. (5) it follows that with equal allowable bearing pressures

$$\frac{n_1}{n_2} = \frac{d_2}{d_1} \quad .. \quad .. \quad .. \quad (6)$$

where d_1 and d_2 are the cylinder diameters. If, to similar cylinders, an equal boost pressure is applied, p_{me} will be approximately the same, and thus with the same c_m, the power per piston area is a constant index value. This value is also a measure of the thermal and mechanical specific speed of the engine. According to eq. (2), Ne/V_h decreases with increasing cylinder dimensions in the inverse proportion of the linear dimensions. In Fig. 1 the ratios Ne/V_h and those of N_e/F are plotted against the ratio of the diameters.

THE POWER OF THE MULTI-CYLINDER ENGINE.

For a given power N_e a certain total piston area F is required, which is to be sub-divided into several individual piston areas. The latter will be smaller the more cylinders are contemplated. Keeping the ratio s/d (stroke to bore) constant, it is clear that the total capacity (volume) becomes smaller the greater the number of cylinders used. Utilizing the greater boost pressure possible with small cylinders the total required piston area can still be reduced, as N_e/F increases, due to higher mean pressure. Without taking this further reduction of total cylinder capacity into account, Fig. 2 shows the decrease of total cylinder capacity with increasing number of cylinders at constant boost pressure. As all the outlines of Fig. 2 are based on constant total piston area the decrease of total cylinder capacity is clearly brought out. Denoting the number of cylinders with Z, the individual piston area is $\frac{\pi d^2}{4} = \frac{F}{Z}$ (m.^{2}), and therefore $d = \sqrt{\frac{4}{\pi} \times \frac{F}{Z}}$ (*m.*). If for simplicity's sake $s = d$, the total cylinder capacity becomes $V_h = F \sqrt{\frac{4}{\pi} \times \frac{F}{Z}} \times 10^3$ (1). This is plotted in Fig. 3 in non-dimensional form, and the ratios shown apply to constant boost pressure.

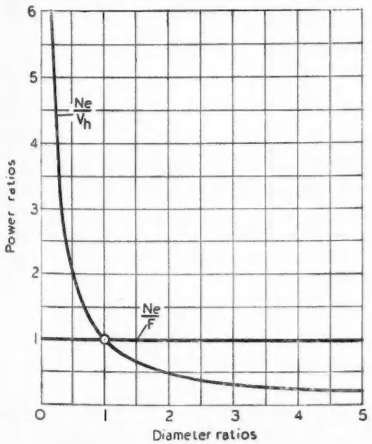

Fig. 1

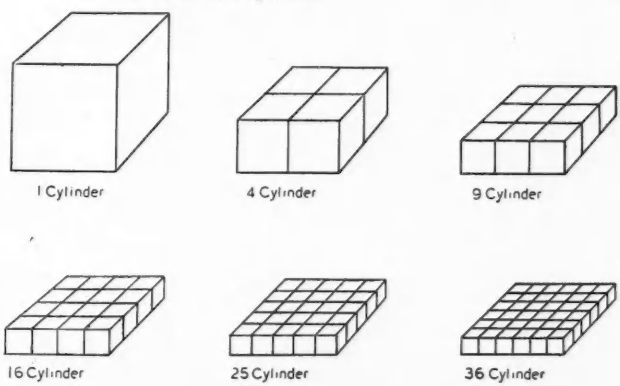

Fig. 2

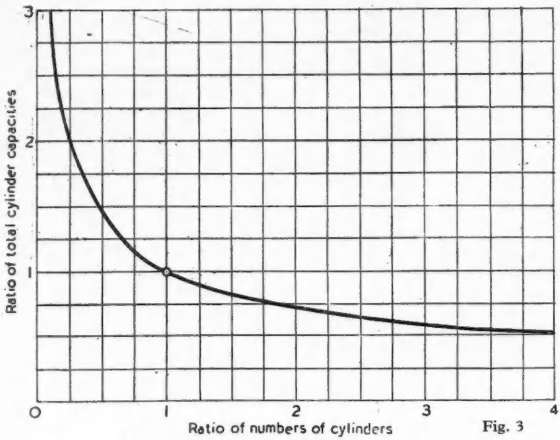

Fig. 3

THE ENGINE WEIGHT.

In weight considerations, too, the piston area is a basis of reference.

If the engine is built of Z equal units, its total weight $G = zG_1$, and the total piston area $F = zF_1$. One can further write (index 1 denoting the unit)

$$\frac{G}{F} = \frac{G_1}{F_1} = \frac{G_1}{V_{h1}} s_1 ;$$ the L.H.S. of the equation decreases with smaller stroke, i.e. with increasing number of cylinders. Accordingly, the power loading

$$\frac{G}{Ne} = \frac{F}{Ne} \frac{G_1}{V_{h1}} s_1 = Cs_1$$

becomes favourable with an increasing number of cylinders. Thus, the small cylinder dimensions are by no means a weight increasing feature; especially as the higher mean pressure of the small cylinder contributes to saving in weight.

CONCLUSIONS.

The development of the aero-engine with present-day large cylinder size, has reached the values of $\frac{Ne}{F}$, which can be compared with those obtained with automobile engines using small cylinders. The decrease in cylinder size is a trend open to the aero-engine designer who, in this way, could also obtain smaller frontal areas per given power, and within certain design limits, a smaller space for his engine.

EXPERIMENTAL DETERMINATION OF THE STRESS CONCENTRATION FACTOR DUE TO AN ABRUPT CHANGE IN THE DIAMETER OF A SHAFT IN TORSION.

By A. WEIGAND, Report of the *D.V.L.*, Berlin. (From *Luftfahrtforschung*, Vol. 20, No. 7, July, 1943, pp. 217-219)

THE stress distribution in shafts in torsion, if the change in diameter is abrupt, has been calculated by F. A. Willers[1] by use of an approximate method of integration. For the case $D-d \geq 2\rho$, Fig. 1, R. Sonntag[2] gave an approximate formula for the stress function and maximum stress. Jacobsen, Thum and Bautz[3] found the stress concentration factor by means of tests based on the analogy between stress distribution and distribution of electric current. The values thus found did not agree with those calculated by Sonntag, a fact which has been discussed by these authors[4].

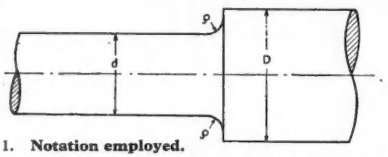

Fig. 1. **Notation employed.**

To achieve final clarity, tests have been made by the present author on steel shafts using the sensitive strain gauge developed by E. Lehr and H Granacher[5], the gauge length of which is 1.3 mm.

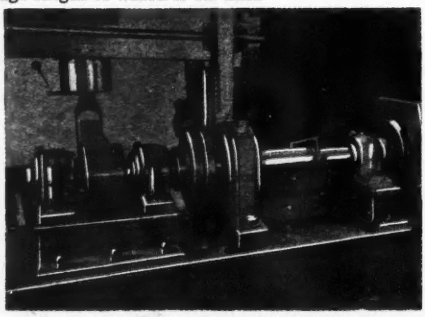

Fig. 2. **Test set-up.**

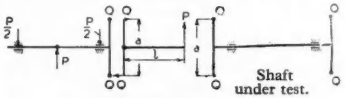

Fig. 3. **Torque (P.l), and its application.**

Fig. 2 shows the test set-up, Fig. 3 is explanatory to it; the shaft is under pure torque. Measurements were made at three points on each of the eleven stations (Fig. 5). The object of the measurements was to determine the two principal strains ϵ_1 and ϵ_2, which must be equal, but of opposite sign.

The three readings taken at I, II and III (see cross-section Fig. 5) have been averaged, and thus the strain values at eleven stations were obtained. The following known relations are used

$$\sigma_1 = \frac{E}{1-\mu^2} (\epsilon_1 + \mu \epsilon_2)$$

$$\sigma_2 = \frac{E}{1-\mu^2} (\epsilon_2 + \mu \epsilon_1) \quad .. \quad .. \quad (1)$$

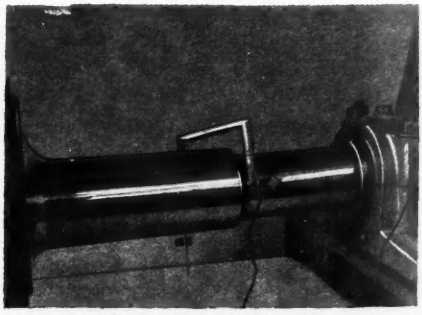

Fig. 4. **Shaft under test with strain gauge.**

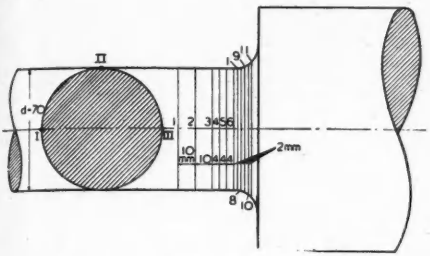

Fig. 5. **Eleven test stations. Test points along three generators (I., II., III.) at 90 deg. to each other.**

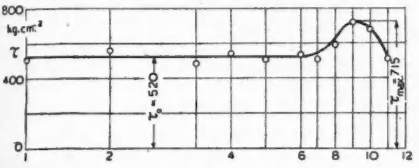

Fig. 6. **Shear stress distribution along shaft showing stress increase at fillet.**

where σ_1 and σ_2 are the principal direct stresses, E is Young's modulus, μ is Poisson's ratio.

The shear stresss is given as

$$\tau = \frac{\sigma_1 - \sigma_2}{2} = \frac{E}{1+\mu} \cdot \frac{\epsilon_1 - \epsilon_2}{2} \quad .. \quad (2)$$

In the present tests $E = 2.14 \times 10^6$ kg./cm.² the shear modulus $G = 0.82 \times 10^6$ kg./cm² and therefore

$$\mu = \frac{1}{2} \frac{E}{G} - 1 = 0.305 \text{ or approx. } 0.3$$

Thus the shear stress becomes

$$\tau = 0.823 (\epsilon_1 - \epsilon_2) \times 10^6$$

For the case $\rho/d = 0.107$, $d/D = 0.70$ the distribution of shear stress along a penetrator of the shaft is plotted in Fig. 6. The fillet begins at station 8, shortly before the stress increases to reach its maximum value at station 9. For this case the stress concentration factor α_k is :

$$\alpha_k = \frac{\tau_{max}}{\tau_0} = \frac{715}{520} = 1.38$$

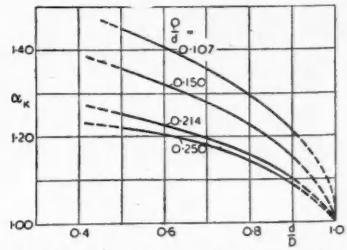

Fig. 7. **Stress concentration factor α_k against d/D.**

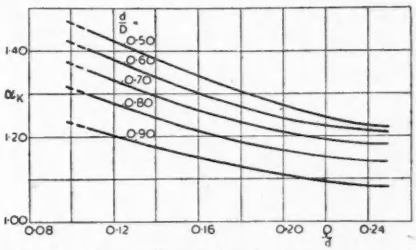

Fig. 8. **Stress concentration factor α_k against ρ/d.**

In the same way a number of tests have been analysed and plotted in Figs. 7 and 8. The values of α_k are consistently somewhat lower than those predicted by the approximate formula of Sonntag :

$$\alpha_k = \beta (1.5 + 3.0\alpha) \frac{1+4\alpha}{1+6\alpha} + (1 - \beta - 2\alpha\beta)\left(1 + \frac{1}{12\alpha}\right) \quad (3)$$

where $\alpha = \rho/d$ and $\beta = d/D \leq \frac{1}{1+2\alpha}$

This experimental investigation has confirmed the validity of Sonntag's formula, with sufficient accuracy, in the intervals $0.1 \leq \rho/d \leq 0.25$ and $0.5 \leq d/D \leq 0.9$.

REFERENCES.

(1) F. A. Willers, *Z. Math. u. Phys.*, Vol. 55, 1907, p. 225.
(2) R. Sonntag, *Z. Angew. Math. u. Mech.*, Vol. 9, 1929, p. 1.
(3) A. Thum & Bautz, *Z. VDI.*, Vol. 79, 1935, p. 1303.
(4) R. Sonntag, A. Thum, W. Bautz *Z. VDI*, Vol. 81, 1936, p. 561.
(5) E. Lehr & H. Granacher, *Forsch. a.d. Ingenieurwesens*, Vol. 7 1936. p. 66.

ELECTRICAL ENERGY CONSUMPTION IN ELECTROLYTICAL PROCESSES.

By DR.-ING. H. WALDE. (From *Die Chemische Technik*, Vol. 16, No. 16, August 14th, 1943, pp. 153-157).

CONSIDERING the manifold activities of the electrochemical and electro-metallurgical industries in Germany, it will be readily appreciated that these industries represent the largest consumers of electrical energy in the country. In addition to energy requirements, enormous amounts of copper, aluminium, and other non-ferrous materials are required in generating machinery and power transmission systems. For this reason, the attainment of lowest possible specific energy consumption in the various processes has been, and must always remain, a paramount task, the importance of which can be gauged from the fact that a general reduction in energy requirements of the German electro-chemical industries by only one per cent would be equal to lowering of the generating capacity requirements by some 10,000 kW.

The efficiency of electrolytical processes is generally expressed by the current efficiency determined as the percentage ratio of the actually produced electro-deposition (per amp. hr.) to that theoretically obtainable according to Faraday's rule. This efficiency does not, therefore, take into account the voltage. But the latter is included in the term " energy efficiency," which is the percentage ratio of the product of (theoretically required number of ampere-hours and the minimum voltage) to (the product of the number of ampere-hours and voltage actually required).

The quest for further improvements of the electrolytical process, therefore, centres around the problems of designing a plant of maximum efficiency, and of operating it in such a way as to maintain highest possible efficiency in continuous plant operation.

Considering the design aspects first, best possible conditions must be obtained with regard to the following points in order to approximate actual cell voltage to the theoretical value : (a) electrodes ; (b) distance between electrodes ; (c) electrolyte ; (d) current density ; (e) temperature ; (f) movement of the electrolyte.

Regarding point (a), it is obvious that the choice of the electrodes must be made in consideration of their chemical composition, surface formation, and electrical

conductivity. For processes operating with indissoluble electrodes, platinum would constitute the most suitable electrode material; but this cannot be considered because of its prohibitive cost. According to process conditions, the choice will therefore have to be made between graphite, lead and its antimony alloys, silver and other metals, magnetite, or, in the case of alkaline electrolytes, also nickel or iron. Frequently the surface contour of the electrodes is of decisive influence upon the attainment of optimum cell voltage. In certain cases, it is also possible to reduce cell voltage requirements by pre-treatment of the electrodes.

Considering point (b), the requirements of minimum cell voltage call for the smallest electrode distance feasible, the attainable minimum distance varying with type and operating characteristics of the process in question. Thus in the electrolysis of metallic compounds care will have to be taken to prevent the growth of deposits to such an extent that they form a bridge between the electrodes or pierce the diaphragm, since this would lead to short-circuiting of the cell. On the other hand, very small electrode distances can be employed in the electrolytic production of gases if provision is made for removing the gases as fast as they are formed.

With regard to point (c), it is clear that the bath resistance should be kept as low as possible by the use of a highly concentrated electrolyte. In certain cases, the addition of conducting salts to the electrolyte may be resorted to.

As a rule, the current density, constituting the factor (d), should be kept as low as practicable by employing large electrode surfaces, unless consideration of secondary reactions or other specific operating characteristics make the use of high current density an essential requirement. Also, large electrode surfaces increase the cost of the cell and the space requirements. Enlargement of the effective electrode surface by mechanical or chemical methods (artificially produced surface roughness, etc.) is often used to advantage.

As far as the temperature of the electrolyte is concerned (e), the decreasing voltage requirements with the temperature should be utilized by employing the highest electrolyte temperature compatible with operating conditions.

The requirements of factor (f) can be met by providing an effective stirring or circulating device; but this frequently proves a most difficult problem.

From the viewpoint of operational efficiency, continued registration and control of amperage, voltage, electrolyte temperature, electrolyte supply and discharge, and analytical supervision of the latter are matters of prime importance. Any process interruptions should be avoided, as even short-time interruptions have an adverse effect upon process efficiency. Other points to be considered are the maintenance of all contact points in clean condition, production of a uniform anode material, prevention of short-circuits, and prompt removal of the cathodes after the required thickness of deposit has been reached.

ELECTROLYTIC PRODUCTION OF COPPER.

The electrolytical production of copper is carried out with an electrolyte of good conductivity, at approx. 55 deg. C., the relatively low current density of 140-180 amp. per sq. m. being employed. The cell voltage ranges from 0.2-0.3 volt, and the current efficiency is 92-94 per cent. In modern plants the power consumption per ton of copper produced usually lies at 270 kW, measured at the cell terminals; but in a few instances, power consumptions as low as 235 kW have been registered.

From the operational point of view, further improvements in the electrolytical production of copper are hardly feasible. Also, it appears more important to aim at a further decrease in cell voltage rather than at a diminution of current efficiency. Even if a further decrease in current efficiency by 5 per cent was attainable, this would lower the specific power consumption by no more than approx. 15 kW per ton of copper; while a diminution in terminal voltage by only 0.05 volt would yield a reduction in power consumption by 42 kW per ton of copper produced.

ELECTROLYTICAL PRODUCTION OF ZINC.

Different conditions prevail in the electrolytical production of zinc, in which the zinc is precipitated from an aqueous solution upon insoluble electrodes, the operating voltage being about ten times that employed in the copper electrolysis. The low power consumption essential for the electrolytical production of zinc calls for a painstaking purification of the electrolyte by means of a highly expensive plant equipment. Further difficulties to be overcome in the attainment of maximum production economy are the opposing influences of the various operational factors upon process efficiency. Thus, it is not possible to treat the current density and voltage as separate factors, and optimum operating conditions must at the least be a compromise. This holds likewise true with regard to the acid concentration of the electrolyte and its circulation speed through the cells. While a high degree of concentration serves to lower the cell potential required, it acts increasingly to cause re-solution of the zinc. In the same manner, a high rate of circulation helps to decrease the required voltage, but tends to favour re-solution. In view of the formidable difficulties encountered, it is not surprising that in spite of 25 years of most active research the technique of the process of electrolytical production of zinc can by no means be considered as having reached its final stage.

The lowest power consumption for the electrolytical production of zinc recorded in literature is 2830 kW-hr. per ton, which corresponds to a current efficiency to 94 per cent. With a measured average cell voltage of 3.25 volts (as compared to a theoretical figure of 2.35 volts) the efficiency of the process approximates to 65 per cent. If converter plant losses are taken into account, and if the energy consumption of auxiliary plant is also included, an overall power consumption approximating to 3500 kW-hr. per ton represents a record figure. From the aspect of energy consumption, the new process, jointly developed by the Duisburg Copper Smelter and the I.G. Dye Trust, deserves considerable interest. In this process, operating with mercury cathodes, the zinc is produced as an amalgam from which zinc of 99.999 per cent purity is recovered with the use of special electrolytical plant, power consumption amounting to 3760 kW per ton, including all electrical losses.

In this process, a zinc-chloride solution is used as electrolyte, hereby producing chlorine as by-product. Making an allowance of 1700 kW-hr. per ton of chlorine produced, the gross power consumption per ton of zinc produced is only 2000 kW. It is, therefore, to be considered that this producer may well assume a pronounced importance.

ELECTROLYTICAL PRODUCTION OF ALUMINIUM.

Unlike the processes considered so far, the electrolytical production of aluminium is carried out with a molten electrolyte at high temperature. Thus a considerable portion of the process power requirements are due to thermal losses by conduction and radiation. In addition to the achievement of optimum current density, efficient thermal insulation is, therefore, highly important. Regarding the former factor, it is interesting to note that the high current density of 64,000 amp. per sq. m. of anode surface, as it was used in the early

plants, has been gradually lowered to 11,000-13,000 amp. per sq. m. Regarding the latter point, that is, the thermal insulation, this is obviously a problem of plant design which calls for the combined efforts of electro-chemist and furnace designer. The progress made in this respect during recent years is illustrated by the fact that in French practice a power consumption of 18,000 kW-hr. per ton of aluminium produced could be recorded in 1935, which compares with a figure of 42,000 kW-hr. per ton required in 1888, the plant amperages being 50,000 and 4000 amp. respectively. But even so, the position remains unsatisfactory if it is considered that the actually required terminal voltage still approximates to four times the theoretical value.

ELECTROLYTICAL PRODUCTION OF HYDROGEN AND OXYGEN.

The electrolytical production of hydrogen and oxygen from an aqueous electrolyte is characterised by the fact that no electrolytical reactions are involved. Compared to other methods of hydrogen production, the electrolytical process excels by the high purity of the product, as any oxygen which may have diffused into the anode space can be easily removed. This high purity is of particular importance in a number of applications. Naturally, the electrolytical production of hydrogen will always be preferred where water power is available. For the last fifty years a large amount of research has been carried out in order to reduce production cost as well as space and material requirements of plant to a minimum. Low production cost is of course of especially vital importance in the development of hydrogenation processes.

Because of the simplicity of the process as such and the absence of complicating secondary effects, the various factors influencing process cost are, to-day, known in every detail, and the achievement of plant perfection has become a mere question of design and material. Since the process of electrolytical water decomposition is carried out with nearly 100 per cent current efficiency, cell voltage and specific power consumption can be adjudged directly on the basis of Faraday's law. Thus, a terminal voltage of 1.8 volt corresponds to an electric power consumption of 4.0 kW-hr. per cu. m. of hydrogen (plus 0.5 cu. m. of oxygen) produced ; while the respective power consumption obtaining with a cell voltage of 2.1 volt amounts to 4.67 kW-hr. Optimum economy will be obtained with a plant combining highest current density and lowest cell voltage with a minimum of space requirements.

Since both the hydrogen and oxygen produced must be compressed for the purpose of transportation, direct electrolytical production of the two gases by the employment of pressure cells appears to be the logical procedure. Investigations showed that such a direct production at high gas pressure does not involve any increase in specific power consumption over the atmospheric pressure process. According to present day knowledge, this phenomenon is due to the fact that the nascent gas bubbles at the electrodes decrease in size with higher pressure, hereby lowering the electrical resistance of the cell. An additional advantage of the high pressure process is that it permits the use of a small electrode distance owing to the small gas spaces at the electrodes required. In experimental plants operating at 60 atmos. pressure and equipped with special electrodes, cell voltages of less than 2 volt have been achieved with current densities as high as 4,000 amp. per sq. m. ; while with a current density of 2,000 amp. per sq. m. a voltage of 1.8 volt has been attained, thus approaching the aforementioned figure of 4 kW-hr. per cu. m. hydrogen produced. Considering that this process saves about 0.2 kW-hr. per cu. m. which would otherwise be required for compressing the gas, this method indubitably offers attractive possibilities for decreasing specific power consumption.

SCALING OF LOCOMOTIVE BOILERS.

By H. ARMAND, Chief Engineer of the S.N.C.F. (From *Revue Générale des Chemins de Fer*, Vol. 62, No. 4, July-Aug., 1943, pp. 73-89.)

IN analysing the problem of boiler scale formation, two principal stages must be distinguished, viz., the appearance of the solid phase in the water and the mechanism underlying the attachment of these solids to the interior boiler surfaces.

With regard to the chemical aspects of scale formation, it is well known that water may contain variable quantities of the salts of sodium, calcium, magnesium, etc., while varying percentages of silica are usually also present. Under the action of heat and evaporation salts are precipitated and form scale.

Scale formation is due to the fact that certain solids are deposited as crystals which, as they grow, form tenacious structures in which other elements are entrapped. These structures are only formed around nuclei of crystallisation attached to the boiler wall. As a matter of fact, they never grow beyond 0.1 mm. thickness. Scale formation is thus bound up with two physical phenomena : first, attachment of the nuclei to the wall ; and, second, growth of scale and maintenance of its compactness.

The phenomenon of nuclear attachment to the wall is easily understood where rough surfaces are concerned, and, other conditions being equal, a rough surface will be encrusted faster than a smooth one. Thus cast iron is encrusted more quickly than sheet metal, and the latter more rapidly than a polished surface. However, roughness is not the sole cause of adherence, and the phenomenon of attraction is the more important. This force of attraction, which is doubtless an electrostatic phenomenon, is exerted by the metallic wall upon the solid particles deposited from the water. It is this electrostatic attraction which explains the adherence of scale to even the most highly polished surfaces, as, for instance, chromium-plated copper. Moreover, these forces of attraction are considerable in themselves, and much stronger than the forces exerted upon the particles by the water circulation. Thus, scale is formed even on surfaces past which the circulation is violent. It can, therefore, be concluded that the adhesion of scale can be prevented neither by improving the nature of the surfaces nor by modifying the circulation of the water. The growth of scale is due to the precipitation of salts which may be caused by the liberation of carbon dioxide, as in the case of feedwater heaters. Or, what is still more important, it may be due to precipitation when evaporation occurs. This, of course, explains why evaporating surfaces become covered with scale much faster than others. Nor does the formation of steam bubbles act to impede the growth of scale, and even the most violent agitation of the liquid cannot suppress the forces of attraction. But when the scale has reached a certain thickness, it becomes increasingly subject to the erosive action of the water currents, actual conditions depending also upon the nature of the scale.

Once the scale is formed, any deformation of the surface to which it adheres will tend to dislodge it. Among the two kinds of deformation to be considered, that caused by a change in the contour of the wall surface is the more important, e.g., in the fire box where the curvature of the walls changes with temperature and pressure. In this case the brittle scale is unable to adapt itself to the change of contour of the

surface, and it is therefore frequently flaked off. The other type of deformation is the linear thermal expansion of the metal. Measurements of the thermal expansion of scale made at the laboratories of the S.N.C.F. have shown that the thermal expansion of scale is only little different from that of steel, scale having an expansion coefficient of $12 \times 10\text{-}^{6}$ as compared to $11\text{–}13.10\text{–}^{6}$ for steel. For this reason thermal expansion alone will not cause the scale to crack off from a steel surface. However, in the case of copper, which has an expansion coefficient of $18 \times 10\text{-}^{6}$, flaking off will occur. This explains why steel fire boxes are more subject to scaling than copper ones. This disadvantage of the steel fire box is further accentuated by the greater roughness of the surface of the steel plate, and by the chemical reactions between scale and steel, which increase the adherence of the scale to the sheet.

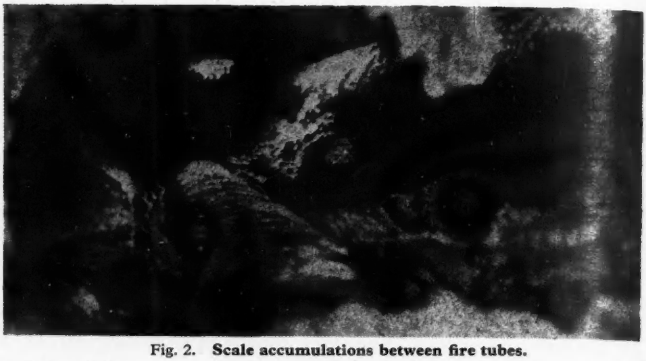

Fig. 2. **Scale accumulations between fire tubes.**

Experience shows that where the scale is flaked off or cracked, the formation of new deposits goes on ceaselessly, even on copper surfaces. If this regrowth of scale could be inhibited, either by the use of pure or treated water, cracking of the scale under the influences of thermal expansion and contraction of the sheet would gradually lead to the dislocation of scale deposits altogether. This de-scaling effect is noted when washing out hot locomotive boilers with cold water. However, because of its harmful effects upon the boiler, this method has been ruled out in favour of chemical de-scaling treatment.

Scaling Troubles Experienced in French Locomotive Operation.

Where the calcium content of the water is high, certain parts of the feed water system become rapidly covered with scale consisting exclusively of calcium carbonate and magnesium carbonate originating from the decomposition of the bicarbonates. Deposits of this type are found in the injectors and internal parts of the boiler feed system, etc. These scale deposits, although not of very tenacious nature, nevertheless build up to considerable thickness on the unheated surfaces of the boiler system where their accumulation is not counteracted by thermal expansion and contraction. The extent to which scale accumulations in the injector interfere with its operation can be gauged from Fig. 1. De-scaling of the injector is effected by its removal and subsequent treatment with acid. Under certain water conditions, cleaning of the injector must be done every 8–10,000 km. if failures are to be avoided.

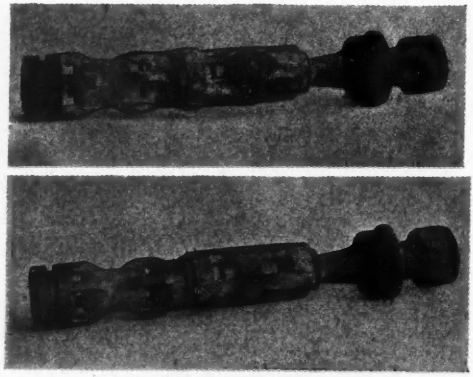

Fig. 1. **Scale-covered injector cone.**

In the case of the feed water heating system, feed pumps are especially affected by trouble of this nature, and, for instance, where Paris water is used, scale removal must be carried out every 15,000 km. This de-scaling is effected by washing with acid solutions to which an inhibiting agent is added. But even so, this process is not without risk, as pieces of scale may become lodged in the valves of the pump.

The feed water heaters or economisers are of tubular construction, the water being preheated to 130 deg. C. prior to its admission to the boiler. Apparatus of this type is particularly prone to suffer from heavy deposits of calcium carbonate. Thus, economisers are useless unless naturally soft water is used or the water is specially treated. It is for this reason that such apparatus have almost entirely lost favour.

The Fire Box.

On the water side of the fire box, as far as it can be thoroughly reached by a jet, only hard scale composed of sulphates or silicates will be found to remain. The fire box surfaces, with evaporation rates as high as 200 kg. per sq. m. per hour, are particularly subject to deposits of calcium sulphate scale, in view of the inverse relationship of the solubility of this compound with the temperature. Incrustations of this kind on the crown sheet may lead to the development of dangerous hot spots. Again, as scale adheres more tenaciously to steel than to copper, scale deposits will make their appearance much faster with fire boxes of steel. Thus, for instance, a steel fire box has been found to accumulate scale 0.5 mm. thick within 15 hours when using hard Marseilles water (of 8 deg. permanent hardness). This scale proved so hard that it had to be chipped off.

Boiler Tubes.

As the gas temperature in the boiler flues varies from about 1,000 deg. C. at the fire box end to about 300 deg. C. at the other end, it can be expected that the nature of the scale deposits will vary over the length of the tube. This is confirmed by the analysis given hereunder, the water being 25 deg. temporary and 6 deg. permanent hardness.

	$CaSO_4$	$CaCO_3$	MgO, SiO_2, etc.
	Per cent.	Per cent.	Per cent.
Fire box end ..	50	24	26
Smoke box end ..	14	59	27

The extent to which scale deposits can accumulate between the tubes is illustrated by Figs. 2 and 3.

While in these parts the thickness of the scale deposits can be kept down, in particular that of carbonate scale, formation of tenacious thick layers of sulphate scale cannot be suppressed, and in the less accessible parts this may reach a thickness of several millimeters.

Moreover, as scale formation occurs rapidly, it cannot altogether be prevented by washing out, as washing out the boiler after every 100 to 200 km. is, of course, not practicable.

With regard to the total weight of scale that may accumulate in the boiler, it is reported that for German locomotives total weights of 700 kg. have been recorded, which is equivalent to a 2 mm. thick scale extending over the whole interior surface of the boiler.

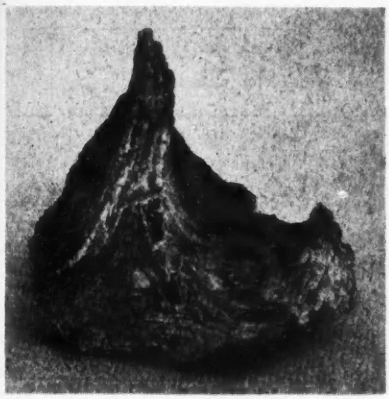

Fig. 3. Typical scale deposit.

The coefficient of thermal conductivity of scale amounts to about $k=2$, which compares with values of $k=50$ and $k=300$ for iron and copper respectively. This means that the temperature difference required to pass the same amount of heat through a layer of scale is 25 times larger than that required in the case of a steel plate of equal thickness, and 300 times larger than with a copper sheet. Practice has shown that the thermal conductivity of scale varies within rather wide limits according to their composition. Thus a dense scale composed of calcium sulphate crystals, arranged perpendicular to the heated surface, has a relatively high thermal conductivity; while a carbonate scale is a less good conductor of heat if it is of heterogeneous structure, or if it has built up in layer-like formation. A still poorer conductor of heat is porous silica scale with a value of $k=0.5$.

Assuming an average conductivity of $k=2.0$, it is easily seen that a very thin layer of scale suffices to double the temperature drop for a given heating transfer. Thus, with a fire box copper plate thickness of 15 mm., a 100 per cent. increase in temperature drop across the plate will be caused by a 0.1 mm. thick layer of scale; while, with a fire box steel plate of 10 mm. thickness, 0.4 mm. of scale will have the same effect. These figures show that the superior thermal conductivity of the copper fire box may be easily cancelled out by scale formation.

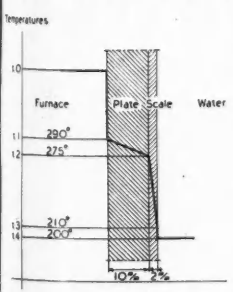

Fig. 4. **Temperature distribution across plate.**

Considering a fire box plate covered by scale on the water side, as shown in Fig. 4, it is easily seen that the temperature drop across the plate can be expressed

$t_1 - t_2 = Q\,\frac{e_p}{k_p}$ where e_p is the thickness of plate and Q is the amount of heat transmitted per unit of surface. As the scale adheres tightly to the plate, the heat flow between plate surface and scale will take place without temperature drop. With a thickness of scale e_t and a respective thermal conductivity k_t, the temperature drop across the scale will be given by $t_2 - t_3 = Q\,\frac{e_t}{k_t}$

The total temperature drop from water to fire-exposed plate surface can, therefore, be found as $t_1 - t_e = Q\left(\frac{e_p}{k_p} + \frac{e_t}{k_t} + \frac{1}{k_s}\right)$ where k_s is the coefficient of heat transfer between water and scale, and t_e is the temperature of the water. The influence of the scale is then given by the ratio $\frac{e_t}{k_t} \Big/ \left(\frac{e_p}{k_p} + \frac{1}{k_s}\right)$. Actually $\frac{1}{k_s}$ will vary between 1/7,000 and 1/1,000, and e_p/k_p will be 1/20,000 for copper and 1/5,000 for steel plate. On the basis of these data, theoretical plate temperatures can be compared as follows:—

	Evaporation kg./sq.m./hr.	Temperature of plate on fire-exposed side	
		Clean plate	Plate covered with 2 mm. scale
Fire box sides (copper)—			
Average rating ..	100	215° C.	280° C.
Maximum rating ..	200	225° C.	350° C.
(k_s = 7,000)			
Fire box sides (steel)—			
Average rating ..	100	225° C.	290° C.
Maximum rating ..	200	245° C.	370° C.
(k_s = 7,000)			
Fire box crown (steel)—			
Average rating ..	100	280° C.	350° C.
Maximum rating ..	200	340° C.	470° C.
(k_s = 1,100)			

This table shows that the high thermal conductivity of the copper is of little influence, and it also shows that the presence of scale causes a rise in surface temperature of 130 deg. C. It should, however, be noted that a computation of this kind does not completely assess the influence of the scale in so far as the real temperatures of the plate must naturally depend upon the type of fire box considered, upon the water circulation, and upon the temperature drop between the gases and the metal, etc. Thus the use of a minimum value of k_s = 1,100 rests upon the assumption that a poor water circulation obtains. However, the temperature increases due to the poor conductivity of the scale (2 mm. thick sulphate or 1 mm. thick silica scale) have been actually observed to occur after 10–20,000 km. But it should be noted that while in itself the influence of scale formation is important enough from the aspect of thermal conductivity proper, it is still more important from the viewpoint of impeded water circulation.

By increasing the metal temperature of the hottest parts of the boiler, additional thermal expansions are caused, the effects of which must also be considered. Taking a boiler of the type shown in Fig. 5, the interior part will be subjected to greater expansion than the outer part, and the difference in the

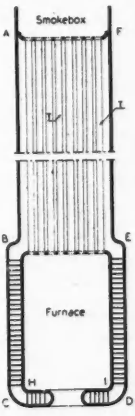

Fig. 5. **Longitudinal section through locomotive boiler.**

expansion of the two parts will be a function of the difference in the respective metal temperatures. Assuming the temperature of the outer metal part to be 10 deg. C. in excess of the water temperature, it can be shown that in the case of a modern locomotive with steel fire box (length of fire-box 2 m., and length of tubes 6 m.) the difference in respective expansions will amount to 5.3 mm. if the surfaces are clean, and to 11.3 mm. if the surfaces are covered with scale. In the case of fire boxes of copper, this expansion differential will be still greater, rising to 14.4 mm.—that is, by 50 per cent. compared to the steel fire-box. It is obvious that expansions of this order must lead to deformation of the various parts of the boiler.

Omitting a theoretical computation of stress and strain imposed upon the various parts, it will be sufficient to state that the front plate *AF* will be deformed less than the hotter fire box tube plate *GI*. The latter transmits the thermal expansion thrust of the tubes to the sides of the fire box *GH* and *GI*. These, undergoing an expansion of their own, will be deformed and transmit the residual thrust to the fire box door plate *HI*, from whence it is passed on through the stays to the outer plate *CD*. It is easily seen that the worst conditions prevail in the case of the tube plate of the fire box, which, because of the tube holes, is not very strong in itself. If made of copper, its strength is also considerably impaired by the prevailing elevated metal temperature. In addition to the longitudinal expansion stresses, there are also present vertical stresses, as thermal expansion will raise the crown sheet by some 0.5 mm. if no scale is present, and by 2 mm. if a scale thickness of 2 mm. is assumed. Furthermore, in the case of the copper fire-box, the stays will cause a deformation of the copper plate, and lead to leakages; while in the case of the steel fire-box, fissures of the plate and breakage of stays are predominant. However, where scale accumulations are absent, the steel fire box must be considered as distinctly preferable to one of copper; and it can be said that the future belongs to the welded fire-box of steel, provided, of course, that the scaling problem is solved.

The influence of scale accumulation upon maintenance can be gauged from a comparison of maintenance hours required for locomotive boilers subjected to scaling, and for such kept clean by the T.I.A. system of internal "integral" boiler water treatment. A number of typical results are given below :—

Depot	Locomotive type	Hours spent on Maintenance per 10,000 km.	
		Boilers with Scale	Scale-free Boilers
Joncherolles (Nord)	141 TC	78	2.8
La Villette (Est)	141 TC	43	14
Avignon (Sud-Est)	231 C	81	7.3
Carnoules (Sud-Est)	140 B	126	13

To judge from a number of runs totalling more than 6 million kilometres with poor quality feedwater, it can be said that on the average 64 hours of maintenance must be spent per 10,000 km. run with scaled boilers, as compared to 12 hours with scale-free boilers. As this method of "integral" treatment is used by the S.N.C.F. only since 1940, no figures with regard to heavy repair work can be given as yet.

With regard to the influence of scale upon boiler efficiency, a survey of past records permits the conclusion that the presence of scale leads to a reduction in efficiency by 5 per cent on the average. To a certain extent the adverse effect of scale is counteracted by the employment of superheat, and it can be assumed that with modern boilers some 25 to 30 per cent of the adverse effect of scale upon fuel consumption is cancelled out by the superheater.

Summarising, it can be said that the presence of scale will cause an increase in fuel consumption by some 10 per cent or more. The suppression of scale formation is, therefore, a matter of paramount importance in locomotive economy and locomotive development. This is now becoming increasingly recognised; and, as recent American figures have shown that a saving of 2,000 dols. per year per locomotive can be obtained by scale-free operation, a general application of "integral" water treatment may well be realised in the near future.

BI-METALLIC PYROMETER.

By E. STUART CLARKE. (From *The Commonwealth Engineer*, Vol. 31, No. 6, January, 1944, pp. 148).

SOME months ago the simple pyrometer described in these notes was developed for a specific job requiring an oil temperature in the region of 225 deg. C. correct to ± 5 deg. C. A mercury-in-glass thermometer could have been used but it was desirable to have a more robust instrument to withstand the rough handling involved.

In a certain gun-building job, one component is heated to 225 deg. C. in a gas-fired oil bath, then screwed and shrunk on to another which is cold. Previously, to measure the oil temperature an expensive and unnecessarily accurate and delicate thermocouple and indicator were used, being thus kept from precise high temperature work for which they were intended.

The thermo-element of the new pyrometer is a bimetallic strip consisting of a 10-in. × 1-in. piece of mild steel plate ground on both sides to $\frac{1}{16}$-in. thickness and extended and pointed to form the indicating needle, to which is secured by brazing at its ends, a 10-in. × 1-in. piece of $\frac{1}{16}$-in. brass. Four $\frac{1}{8}$-in. diam. round head screws hold the steel and brass together and prevent bowing at temperature. This element is mounted on a simple frame which carries a dial over which the pointer moves. The instrument is suspended in the oil so that the bi-metallic strip is immersed by some 3-in.

Calibration of the pyrometer was carried out against a standard instrument in an oil bath, the scale being found to be linear and in close agreement with the calculated division of 100 deg. C. per inch of scale.

Oil fires and fumes have disfigured the carefully graduated dial and now a workmanlike file groove marks the mean working temperature. There are no working parts in the instrument which is very robust. The cost of manufacture was about 10/-, and after being in use for more than six months the calibration is unchanged.

This type of pyrometer may have other applications for the measurement of air and liquid temperatures up to about 300 deg. C., and its sensitivity could be made to suit any particular temperature range by altering the thickness of the bi-metal strips.

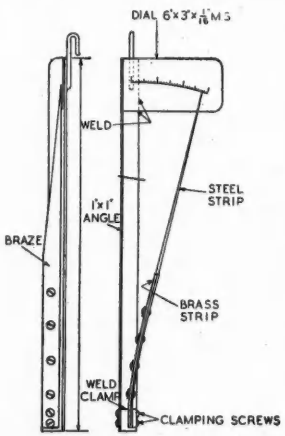

Fig. 1.

INSPECTION OF SPARKING PLUGS AS A MEANS OF CHECKING ENGINE OPERATION.

By WALKER SCHAUER and H. BRUDER. (From *ATZ-Automobiltechnische Zeitschrift*, Vol. 46, No. 11-12, June 25th, 1943, pp. 277-282).

A FUNDAMENTAL condition of reliable engine operation is that the type of engine and the sparking plug be in harmony; pre-ignition is frequently caused by overheated plugs, while too low a plug temperature permits collection of an excessive amount of oil and carbon deposit on the plug and leads to ignition failure. As a general rule, the insulator should assume a temperature of about 500 deg. C. which is called the self-cleansing temperature. This ideal condition cannot always be maintained, for instance, when travelling down hill with fully closed throttle. Under such circumstances the functioning of the plug will be influenced by the general engine condition, e.g., piston clearance, lubrication, etc.

According to temperature conditions prevailing in the combustion chamber, the sparking plug will assume different appearances and typical plug "faces" can be recognised. The appearance of the plug thus provides an additional means of checking engine operation, provided that the following rules be observed.

(*a*) Before inspecting the plug the engine should be run at normal speed and load for at least 25 hours on the test bench, or for 1,000 hours on road runs.

(*b*) Following this test, the engine should not be run with light load or at an idling speed for any appreciable length of time, before the plug is inspected.

FACTORS AFFECTING THE APPEARANCE OF SPARKING PLUGS.

The appearance of a sparking plug is predominantly affected by deposits of various kinds of solid material which may or may not be oil contaminated. The main causes of deposit formation are the following :—

(1) Due to cylinder wear, small oxidised iron particles are carried into the combustion chamber where they are deposited on the combustion chamber wall and the sparking plug insulator. This type of deposit is identified by the typical brownish colour of the insulator and is harmless as regards engine operation.

(2) Small quantities of oil are inevitably carried into the combustion chamber past the piston, and if the plug temperature is under 500 deg. C., some products of incomplete combustion are deposited on the sparking plug. This type of deposit is also harmless if the low temperature prevails for short periods only.

(3) Depending on the mixture strength the fuel itself may yield a residue due to incomplete combustion. This is particularly the case with leaded fuels. The anti-knock additive used at present is lead-tetra-ethyl. During combustion, the lead becomes lead-oxide which is solid at the temperature of combustion. For this reason ethylene-dibromide or ethylene-dichloride is also added to the fuel—which combines the lead-oxide to lead chloride or lead bromide. All the products of combustion are now gaseous and should, therefore, be swept out of the cylinder during the exhaust stroke. Unfortunately, the reaction is not complete, and a small amount of lead oxide and also some lead sulphate is left inevitably in the cylinder. This forms a deposit on the plug, valves and cylinder walls, and is a powder at low plug temperature, but at higher temperatures it melts and forms a glass-like coating. At temperatures above 400 deg. C. the deposit becomes a conductor of electricity and shorts the plug electrodes. In the powder form, the deposit absorbs water at low temperatures and causes starting difficulties. Leaded fuel may also corrode the electrodes (Fig. 1–3).

Another type of anti-knock additive is iron carbonyl which produces a red powder deposit on the plug. As the quantity needed is about twice that of lead-tetra-ethyl, the deposit is also correspondingly heavier. On the other hand, this type of deposit does not adhere so firmly to the insulator as lead oxide, and does not cause corrosion. Iron carbonyl is not used frequently nowadays and its importance is, therefore, only secondary.

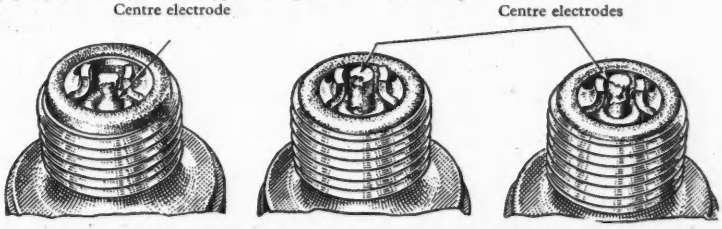

Fig. 2. **The heat conduction of the ground electrode is usually better than that of the centre electrode. Corrosion may progress in many forms as shown in the picture. Elimination of such plug failures is one of the chief aims of plug design.**

Fig. 1. **High operating temperature promotes the corrosive action of leaded fuel. The picture shows a badly corroded ground electrode used in an engine run on leaded fuel.**

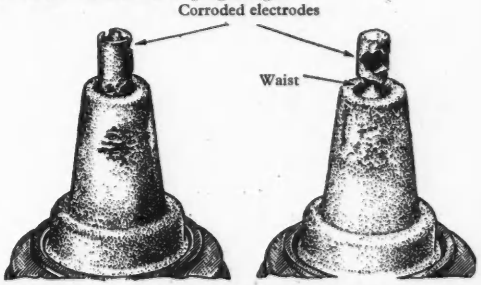

Fig. 3. **Two centre electrodes badly corroded by leaded fuel. Formation of "waist" is characteristic of lead deposit on top of insulation.**

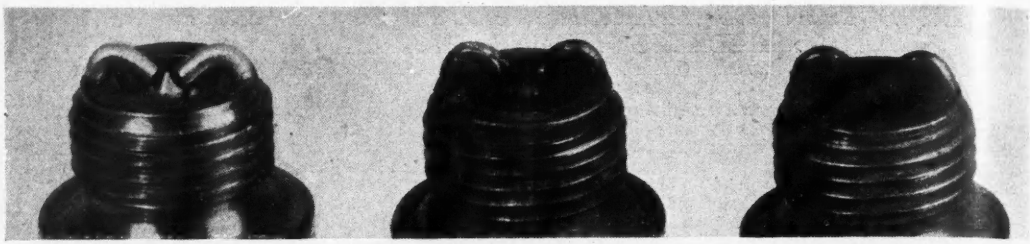

Fig. 4. **Tar deposit on electrodes due to inefficient filtering of producer gas. Left : new plug ; centre : deposit starts to build up and leads eventually to complete failure of plug ; right : engine troubles may also be expected, such as gumming of valve seats, deposit in suction pipe, etc.**

(4) In gas or producer-gas engines, thorough filtering of the fuel is essential. The deposit consists mainly of particles of sulphur and tar, and in producer-gas engines burning charcoal, acetic acid is also formed. Ash and potash are also found on the insulator and, since these substances are highly hygroscopic, starting troubles are frequently encountered.

(5) Atmospheric impurities may also cause deposits on the plugs. With the exception of small 2-stroke engines, no serious consequences are attached to this type of deposit. As the deposit is composed mainly of small particles of lead, iron, or carbon, they may bridge the electrodes of small 2-stroke engine plugs, provided that certain engine conditions prevail. The phenomenon is not yet fully understood, but it seems to be related to an inhomogenous electric field existing between the electrodes at the instant of sparking. It is assumed that metallic or carbon particles are drawn into the electric field from the surrounding atmosphere and are deposited on the electrodes. The trouble may be partly overcome by cleaning the inlet air, frequently cleaning the plug, or by increasing the gap between the electrodes. In the latter case, however, the efficiency of the plug may be reduced.

In the following, some typical plug appearances are discussed. It should be remembered that a multitude of factors affect the appearance of the plug, and therefore, no comprehensive study is intended or could be given. A careful study of typical cases may be helpful, however, in recognising slight modifications and associating them with certain engine conditions.

A.—Well selected sparking plug. Engine condition and mixture strength satisfactory.

This diagnosis applies to liquid fuel engines if the plug insulator shows a light-brown or dark brown

Fig. 5. **Plug in very good condition, no chemical knock prohibitor added to fuel.**

Fig. 7. **Plug used with fuel containing iron carbonyl.**

Fig. 6. **Plug face with leaded fuel.**

Fig. 8. **Corrosion caused by overheating ; liquid fuel contained no knock prohibitor.**

Fig. 9. **Plug removed for inspection too early.**

Fig. 10. **Overheated plug corroded by leaded fuel.**

Fig. 11. **Plug covered with unburnt carbon deposit.**

Fig. 12. **Plug covered with unburnt lubricating oil and carbon deposit.**

colour. The electrodes are of a grey colour, and the plug body is dry or covered with a thin layer of soot (Fig. 5).

With leaded fuel the insulator in this case is dry, greyish yellow or brown; the deposit is a powder and can be wiped off easily. The electrodes show no sign of chemical attack but, similar to the insulator, may be covered with a thin layer of powder deposit. Fig. 6 is a typical plug for leaded fuel, except for the chemical attack shown on the electrodes. A light fawn leaf-like deposit is a lead compound. It is an indication of relatively high content of ethyl or of a rich mixture strength.

Fig. 7 is a typical plug which was used in an engine run on fuel containing iron carbonyl.

B.—Too high plug temperature caused either by unsuitable selection of plug, or by weak mixture strength, or by any other engine condition resulting in high combustion temperatures.

This condition is indicated by a dry, fawn or white insulator, while the electrodes are corroded to a greater or lesser degree and are burnt at the points of sparking. (Fig. 8). A very similar appearance of the insulator is also characteristic of one which has been running for a very short time only, under satisfactory conditions (Fig. 9). These two cases must be carefully differentiated from each other.

With ethyl fuels a dark brown—almost black—deposit forms on the tip of the insulator. This deposit adheres very firmly to the insulator and in many cases it melts and forms small glass-like beads. The electrodes are corroded and usually burnt to a greater extent than with unleaded fuel.

If the trouble cannot be remedied by altering the mixture strength, a plug of higher heat capacity should be tried.

In producer-gas engines, the control electrode is often corroded, though the colour of the insulator is normal. The trouble is usually due to attack by acetic acid or sulphur compounds. In this case, too, the remedy is often found in using a plug of higher heat capacity, since the chemical attack is slowed down at lower temperatures.

C.—Ignition failure due to low plug temperature caused by too rich mixture or by excessive oil leakage into the combustion chamber.

If the plug does no treach the self-cleansing temperature, soot deposits on the insulator and the plug body, forming a black, velvety coating (Fig. 11). In some cases it might also be contaminated by oil. With leaded fuel, a powder deposit collects at the bottom of the insulator, black or greyish black in colour. The electrodes are usually sound.

Fig. 12 shows a plug completely covered with a mixture of oil and carbon. This, too, is caused by too low plug temperature, and if the trouble is observed only after a period of satisfactory operation, it is an indication of too rich a mixture strength.

The deposit is harmful to the insulator only, and if correct operation cannot be restored by altering the mixture, or by reducing the lubricant reaching the combustion chamber, a plug of lower heat capacity should be tried.

THE EXTINCTION OF THE ARC IN SINGLE AND MULTIPLE BREAK AIR-BLAST HIGH SPEED CIRCUIT BREAKERS.

By H. THOMMEN. (From *Brown-Boveri Review*, Vol. XXIX, No. 11/12, November/December 1942, pp. 336-338).

ONE of the most striking features of air-blast breakers with hollow contacts is that the capacity of the hollow contacts not only depends on the nozzle diameter and the air pressure, but also on the travel of the contacts. The capacity, however, does not rise uniformly with increasing contact travel, but approaches an optimum value and then diminishes rapidly if the distance between the contacts becomes still greater. (Fig. 1).

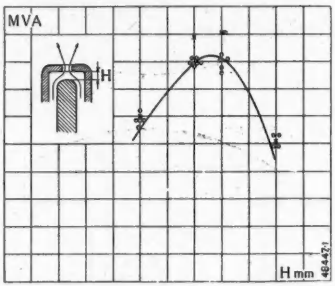

Fig. 1. **Rupturing capacity of a hollow contact in relation to the gap.**

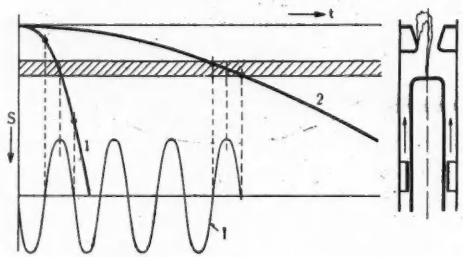

Fig. 2a. **Curve 1 shows that when the arcing contact moves too quickly it is already beyond the arc extinction zone at the passage of the current through zero, while when moving slowly (curve 2) favourable extinction conditions obtain at the moment of passing of the current through zero, but the arcing time will be long.**

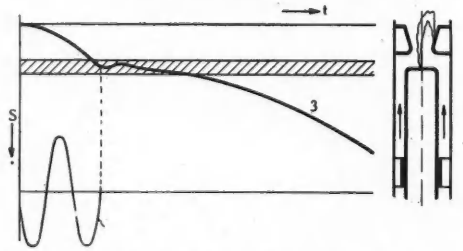

Fig. 2b. **Circuit breaker with irregular contact movement.**

But this most favourable extinction distance is too small to give sufficient electric strength between the contacts when the stream of air ceases. Therefore, a continuous opening movement of the contacts, as is usual with other types of circuit-breakers, is quite unsuitable here (Fig. 2a). These difficulties are avoided if the contact is moved rapidly into the extinction zone, made to remain there for several half-cycles and then moved on. But the design becomes complicated (Fig. 2b).

Another simpler and successful solution consists in sub-dividing the rupturing operation in two separate movements, that of the arcing contacts and that of the disconnecting contacts (Fig. 2c). The travel of the arcing contact is limited so that the most effective extinction zone is utilized, and the very small mass of the contact allows a high speed and extremely short arcing time. The opened disconnecting contact forms a reliable insulating gap.

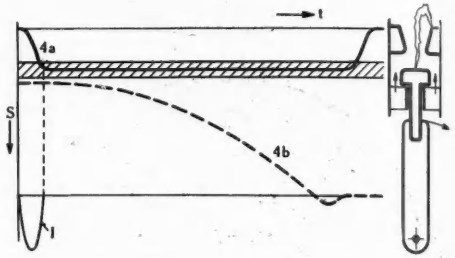

Fig. 2c. **Curve 4a : Movement of arcing contact ; curve 4b : Movement of disconnecting contact.**

Fig. 2. **Influence of movement of arcing contact on arc extinction capacity and arcing time.**
Hatched section : most favourable arc extinction zone. t. Time. S. Contact travel. I. Current.

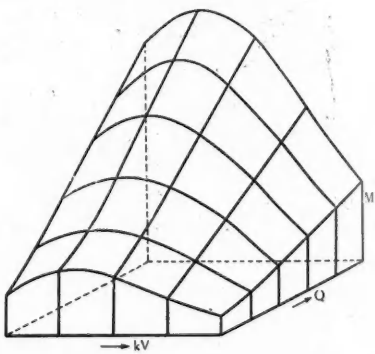

Fig. 3. **Admissible rupturing capacity of air-blast hollow contact in relation to nozzle cross-section at various service voltages.**

This system proved particularly valuable for extra-high-voltages, where by using a potential controlled multiple break mass and travel of the arcing contacts could be further reduced. The connection of several breaks in series gives the arcing contacts a high electric strength. The characteristic feature of circuit breakers with potential-controlled multiple break is that each individual break interrupts a definite, pre-determined power. For this reason, by dealing with one break at a time, circuit-breakers of the highest rupturing capacity can be tested in the existing test bays.

An interesting fact disclosed by a large number of tests (Fig. 3) is that the efficiency of a certain cross-

section Q is greatest at a quite definite voltage range. This can also be proved theoretically.

The air-blast high-speed circuit-breaker is particularly adapted to high-speed reclosing, due to the blast of air rapidly evacuating the gas generated between the contacts.

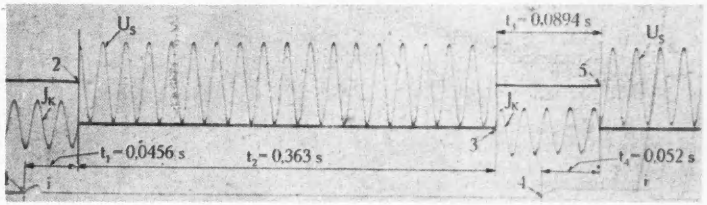

U_s. voltage across circuit breaker contacts. J_K Short-circuit current. i. Current in trip coil. t_1. Rupturing time at first opening operation. t_2. Reclosing time. t_3. Duration of short-circuit current after reclosing. t_4. Rupturing time at second opening operation.

1. Voltage impressed on trip coil. 2. Switch interrupts short-circuit current. 3. Moment of reclosing. 4. Second tripping impulse imparted to trip coil (due to short-circuit persisting). 5. Circuit-breaker opens definitively.

Fig. 5. **Oscillogram of rupturing operation and subsequent reclosing on a dead short-circuit with an air-blast high-speed circuit-breaker for 300 kV maximum service voltage.**

WATER CIRCULATION IN BENT-TUBE AND RADIANT BOILERS.

By DR. ING. M. LEDINEGG. (From *Die Wärme*, Vol. 66, No. 14, April-May, 1943, pp. 111-119.)

WITH higher operating pressures, boiler circulation is known to become slower and less stable. Slow circulation in itself is not dangerous as long as the steam bubbles formed are removed from the heated surfaces. But dangerous conditions arise in the case of unstable circulation, to which sluggish circulation is a contributory factor. From the aspect of circulation, side wall water tubes are more endangered than those on front and rear wall of the furnace, provided the steam-water mixture is passed into the steam space of the drum, thus preventing a reversal of flow.

Mathematical treatment of the factors bearing upon circulation reversal meets with no insuperable difficulties, as has been shown by the author on a previous occasion* when the specific weight of a steam-water mixture was given as

$$\gamma = \gamma_w \frac{F_w}{F} + \gamma_D \left(1 - \frac{F_w}{F}\right) \quad .. \quad .. \quad (1)$$

In this equation, F_w is the tube area occupied by the water, F is the tube area, and γ_w and γ_D are the specific weights of water and steam respectively. It is

$$\frac{F_w}{F} = \frac{\mp A + B \pm 1}{2} \left\{ \pm \sqrt{\frac{\left(\mp A + B \mp 1\right)^2}{4}} \pm B \right. \quad (2)$$

The top range of signs of operation applies with both water and steam flowing upwards; the middle row applies to downward flow of both media, and the bottom row refers to cases in which upward flow of steam is accompanied by downward flow of the water. It is also

$$A = \frac{D}{F\,\gamma_D\,W_r}, \quad B = \frac{G_w}{F\,\gamma_w\,W_r}$$

where G_w and D are the flow rates per second of water and steam respectively at the point considered. The relative velocity W_r of the steam bubbles decreases greatly with increased pressure. It is stated by E. Schmidt† that, according to the load, W_r amounts to 0.25 – 0.5 m. per second with 40 atmos. pressure, and to 0.1 – 0.3 m. per second at 100 atmos. For the particularly important high pressure circulating problems, it is, therefore, frequently possible to assume $W_r \cong 0$. It is thus $\gamma = \dfrac{1}{v_w + \dfrac{D}{G}(v_D - v_w)}$ (3) where v_w and v_D are the specific volumina of water and steam respectively, and $G = G_w + D$ is the total weight passing through the flow area per second.

Generally, the static pressure exerted by a steam-water column is given by $\Delta p_{st} = \int_0^H \gamma \, dx$ (4) where γ changes as the evaporation proceeds over the tube length. Up to $\gamma/\gamma_w \cong 0.5$ it can be written with sufficient accuracy: $\Delta p_{st} = \gamma_m H$ (5) where γ_m is an average value taken over the tube length to be computed on the basis of equations (2) and (3) with the introduction for D only of one-half the steam quantity actually formed. The latter may be expressed by the term D_o in order to avoid the occurrence of errors. Equation (3) can then be written

$$\Delta p_{st} = H \frac{1}{v_w + \dfrac{D_o}{G}(v_D - v_w)} \quad .. \quad .. \quad (6)$$

The frictional pressure drop is given by

$$\Delta p_R = \frac{\lambda}{2g} \cdot \frac{G^2 . L}{d . F^2 . \gamma_m} \quad .. \quad .. \quad (7)$$

where λ is the friction factor, d is the inside tube diameter, F is the internal tube area, L is the tube length, and g is the gravitational constant. If the relative velocity of the steam bubbles is to be considered, values for γ_m must be computed from equations (1) and (2), replacing D by D_o.

A comparison of the friction factors established by Zimmermann* with corresponding values established on the base of Fritsche's friction factor is given below. In the opinion of the author, the latter values vary in undue measure with the weight flow through the tube. It is, therefore, suggested to use the λ values, which can be considered as constant within a wide range of flow rates. Where accurate computation of the circulation is required, the pressure losses at tube inlet and outlet as well as those occurring in the tube bends must also be computed. Their influence may be considered by multiplying the frictional pressure drop by a factor f. The total pressure difference for a tube of the length L

* M. Ledinegg: "Instability with Natural and Forced Circulation," *Wärme*, Vol. 48, 1938, p. 891.

† E. Schmidt: "Water Circulation Experiments," *A. f. Wärmewirtsch*, 1933, p. 1.

* Zimmermann: "New Findings Concerning the Pressure Drop in Straight Risers," *A. f. Wärmewirtsch*, 1940, p. 133.

with its ends having a difference in level H is thus given by

$$\Delta p = \Delta p_{st} \pm \Delta p_R \,.\, f = H\left[\gamma_m \pm \frac{f \,.\, \lambda \,.\, L}{2g \,.\, d \,.\, F^2 \,.\, H} \,.\, \frac{G^2}{\gamma_m}\right] \quad .. \quad (8)$$

the positive sign applying to upward, and the negative sign to downward flow of the mixture.

APPLICATION TO COMPUTATION OF CIRCULATION.

For the investigation of circulation problems, it is most instructive to chart equation (8) in the manner shown in Fig. 1, where the left-hand side of the diagram refers to down-comers, and the right-hand side to risers. The evaporation D is assumed as constant, the weight of steam is taken as the average quantity passing through the tube area at half the height of the tube. The average flow rate of water is determined in identical manner. Curve 2 in Fig. 1 has two asymptotic branches expressing the static head $H \,.\, \gamma_m$. While curve (1) of the riser has a steadily rising tendency, that of the down-comer possesses a maximum with a subsequent decline. For an average steam production $D \leq F\,\gamma_D\,W_r$, the characteristic of the riser is given by curve (3), which indicates that with ascending steam the water flows downwards.

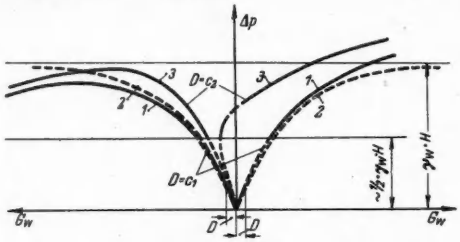

Fig. 1. Pressure drop characteristics of a boiler tube.
Left-hand side, downcomer ; right-hand side, riser.

To each tube or tube row of the boiler circuit a certain evaporation rate is co-ordinated, which may here be considered to be solely determined by the load. By plotting the Δp curve for each of the tubes, a family of curves is obtained as indicated in Fig. 2. The possible

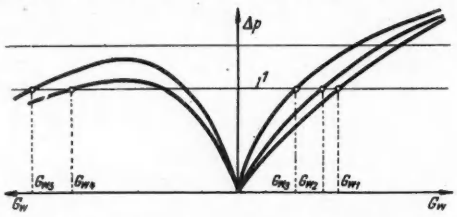

Fig. 2. Determination of water circulation.
Left-hand side, downcomer ; right-hand side, riser.

operating points can then be established by drawing a line 1 parallel with the abscissa intersecting each one of the curves, thus co-ordinating a certain steaming rate G_{w1}, G_{w2}, etc., to the individual tubes. Actually, the location of this intersecting line must be so chosen that the total weight of flow through the riser tubes equals that of the flow through the down-comers. A similar diagram applying to the tubes of a water wall is given in Fig. 3. As all tubes are both parallel and assumed to be uniformly heated, their characteristics are represented by a single curve (4). If the intersecting parallel is represented by line (1) corresponding to a pressure difference Δp_0 between upper and lower water wall header, no flow reversal will occur in any riser. But

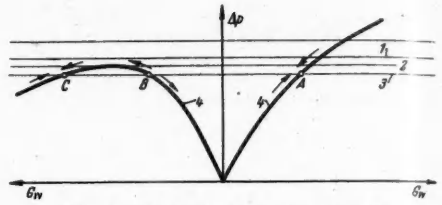

Fig. 3. Water circulation in water wall.
Left-hand side, downcomer ; right-hand side, riser.

should the pressure difference correspond to the lines (2) or (3), a single reversing impulse may cause one of the riser tubes to become a down-comer. Stability of operation can therefore be judged from the pressure difference Δp_0 and from the maximum pressure difference Δp_{max} of the characteristic curve of the down-comer. By writing equation (8) in the form

$$\frac{\Delta p}{H} = \gamma_m - \frac{C^1}{F^2} \,.\, \frac{G^2}{\gamma_m} \quad .. \quad .. \quad (9)$$

the analytical expression for $\Delta p/H$ is obtained as

$$\frac{\Delta p}{H} = f\,(G, D, \gamma_w, \gamma_D, w_r, C^1, F) \quad .. \quad (10)$$

which is graphically represented by Fig. 4. The

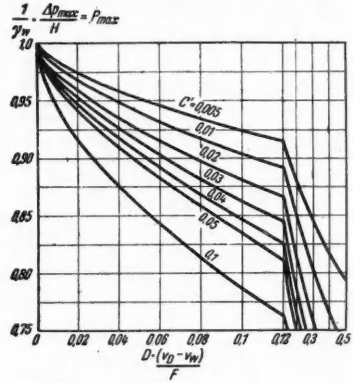

Fig. 4. Graph for the determination of the maximum pressure difference in downcomers.

ordinate of this chart shows $\frac{\Delta p_{max}}{H \,.\, \gamma_w} = P_{max}$ being based on a column of water at the boiling point, corresponding to 100 atmos. Since P_{max} varies only a little with w_r, the chart remains applicable to pressures as low as 40 atmos. In Fig. 5 it is shown that in the case of unequal heating of the tubes, the characteristic of the less heated tube 2 lies above that of tube 1 which is subjected to average heating. With the pressure drop corresponding to the line 3, riser (1) will be stable, while

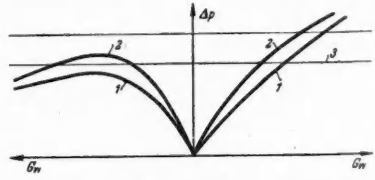

Fig. 5. Characteristic curves for different heat absorptions.
Left-hand side, downcomer ; right-hand side, riser.

flow reversal in riser (2) may occur. When using the graph Fig. 4, P_{max} should, therefore, be determined on the basis of the smallest heat load occurring, and not on the basis of the average heating load; also this P_{max} value should lie below the actual pressure difference P_o between upper and lower water wall header.

The case of unequal flow resistance in the tubes is represented by Fig. 6, where curve (1) is the characteristic of the tube with the smaller, and curve (2) that of the tube with the greater flow resistance. The graph clearly shows that in a water wall composed of tubes of different flow resistance the risers with the smaller flow resistance will tend to show reversal of flow. A uniform increase of the flow resistance of all tubes will depress the maximum value of the characteristic, thus increasing stability of flow. This effect is sometimes realised by inserting orifices at the lower ends of the water wall tubes in order to effect stabilisation of flow.

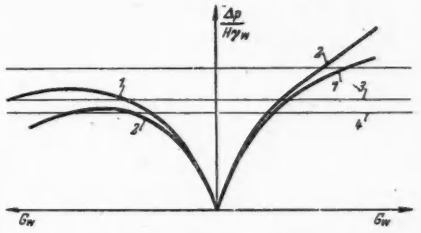

Fig. 6. Characteristic curves for different frictional resistance. Left-hand side, downcomer; right-hand side, riser.

STAGNATION.

At low load, it can happen that owing to insufficient lift, the flow ceases in risers discharging into the steam space of the drum, as shown in Fig. 7. This leads to excessive concentration and scale deposition in the affected tube. Considering tube 3 of the bent-tube drum boiler circuit shown in Fig. 7, water circulation will cease when the evaporation in the tube equals the water supply. Under this condition, the level at the steam-water column will be at H^1. In the computation of γ, a value of $G_w \cong 0$ is permissible in equations (1) and (2). The pressure differential of the steam-water column if found as

$$\Delta p = \left[\left(1 - \frac{D}{F\,\gamma_D\,W_r} \right)(\gamma_w - \gamma_D) + \gamma_D \right] . H^1$$

indicating a linear relationship between Δp and the evaporation D, as shown in Fig. 8. Curve (2) is

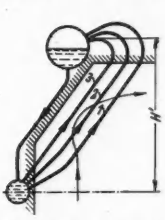

Fig. 7. Bent tube two-drum boiler with external downcomers.

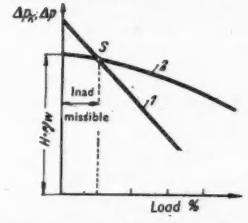

Fig. 8. Determination of load at which natural circulation ceases.

obtained by computing the pressure difference Δp_o prevailing between upper and lower drum with different loads. For no load it is, of course, $\Delta p_o = \gamma_w . H$. The point of intersection S indicates the minimum load at which circulation through the tube still takes place. This shows that with risers discharging into the steam space in the manner indicated, the boiler should not be operated for any considerable length of time at ratings below the limiting load point.

THE INFLUENCE of DIAMETER upon the PROPERTIES of STEEL CABLE.

By W. PÜNGEL, E. GEROLD and A. BEIDERMÜHLE. (From *Zeitschrift des VDI*, Vol. 87, No. 31/32, Aug. 7, 1943, pp. 493-497).

CABLES for mine hoists are generally made of drawn carbon steel wire of about 3.6 mm. diameter with tensile strengths ranging from 100 to 200 kg. per sq. mm. On German mine hoists, wires exceeding 200 kg. per sq. mm. in strength are not used, but these have found an increasing application in recent years in the mine hoists of other countries, particularly in Belgium. The cable loading is usually determined as the static load in direct tension, dynamic and bending stresses being neglected. According to experience, the greatest bending stress occurs only in a limited portion of the cable where they may lead to premature fracture of the wires. For this reason, cable drums of adequate diameter are employed, records being kept of the number of wire fractures occurring during service life.

In mining practice it was further observed that cables of "soft" wires of 140—160 kg. per sq. mm. tensile strength give better service than that of "hard" wires of 160—180 kg. per sq. mm. strength. This observation has since been confirmed by fatigue tests which show that under equal conditions the service life of steel cables under static load decreases with increasing tensile strength. Because of increased cable diameter and, consequently increased cable weight attending the use of soft wires, it is, however, almost always necessary to employ wire of higher tensile strength.

Investigations published so far have been based mainly on cables of equal diameter. The purpose of the present investigation has, however, been to ascertain the influence of cable diameter upon ultimate tensile strength for different diameters of the cable sheave; while fatigue tests with the same cables were also conducted.

Referring to Fig. 1, which shows a cable with one end fixed at A and led over a sheave of diameter D, enclosing the angle α, it can be assumed that the maximum load P which can be sustained will be smaller than the tensile strength of a straight cable, if the diameter D is below a certain limiting value. The assumed diminution of P as compared to the case of direct tensile loading will be essentially dependent upon the diameter D and upon the arc of contact. Theoretically the worst case will occur if the arc of contact should be 180 deg., and if $D = 0$. Conversely, bending stresses will decrease with increasing values of α and D, until an optimum condition is reached in which the tensile strength of the cable reaches that of the cable in direct tension. In this respect, the ratio "cable diameter/sheave diameter" is of special importance.

TABLE I. **Type and Strength of Cables Tested.**

Cable Dia. mm.	Material	Wire Dia. mm.	Tens. Strength of wire kg sq. mm.	No of wires	Ult. Tensile Strength of the cables in direct tension. tons	kg sq. mm.
6.3	soft wire	2.10	92.0	7	1.8	72.5
10.5	,, ,,	2.10	93.0	19	5.45	81.7
14.7	,, ,,	2.07	93.0	37	10.85	86.8
18.9	,, ,,	2.08	94.6	61	18.3	88.0
7.5	hard wire	2.5	162.0	7	5.25	147.7
12.5	,, ,,	2.5	164.0	19	14.7	155.5
17.8	,, ,,	2.5	164.0	37	26.7	146.0

Relevant data on various cables tested are listed in Table I. Only cables composed of hot-galvanised

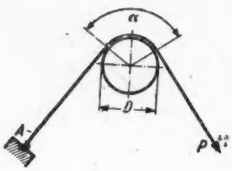

Fig. 1. **Cable subjected to static tensile load and bending stress.**

wires were tested. The two test arrangements used are shown in Figs. 2 and 3, showing a straight and a crossed loop respectively. The tests to fracture were conducted in a tensile testing machine of 100 tons max. capacity. Four different sheave diameters of 200, 150, 100, and 50 mm. were employed, the centre-to-centre distance between the sheaves being 520 mm. in all cases. The different arcs of contact obtaining with crossed loops are given in Table II.

TABLE II.
Arc of Contact. Cables Tested in Crossed Loop.

Diameter of sheave D, mm.	Arc of contact α, deg.
50	194
100	202
150	214
200	226

Several fracture tests were made with each diameter of sheave in order to ascertain its effect upon relative cable strength. The results obtained, charted in Figs. 4 and 5, show ultimate tensile strength expressed as percentage of direct tensile strength versus diameter of the sheaves. Assuming straight-line proportions, the characteristics obtained were extra-polated to extend to larger sheave diameters thus permitting the establishment of probable strength values with sheave diameters up to 350 mm. While with the straight loop (Fig. 4), fracture occurred in every case in the unsupported part of the loop between the sheaves, fracture in the cross-over arrangement (Fig. 5) was found to occur nearly always in that part of the cable contacting the sheave.

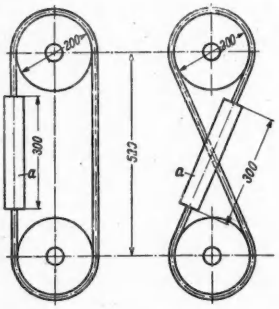

Fig. 2. **Straight cable loop**

Fig. 3. **Crossed cable loop.**

As was expected, the ultimate tensile strength decreased with decreasing sheave diameter. It did not, however, appear feasible to compute the bending stresses on the basis of the data obtained; and evaluation of the latter was therefore limited to determination of the smallest sheave diameter at which the ultimate strength of the loop still equals ultimate strength in direct tension. These data are listed in Table III. and charted in Fig. 6. (For the sake of convenience, these data are given on the basis of the ratio D/d in place of the aforementioned ratio d/D). Referring to the latter chart, it will be seen that for cables of soft wire stressed in straight-loop arrangement (Fig. 2), a sheave diameter of at least 17 times the cable diameter is required if the strength of the looped cable is to equal that obtaining in direct tension. But if hard wires are used, an average value of D/d, approximating to 21, must be chosen. In the latter case also, the cable diameter is seen to be of greater influence than that prevailing with soft wires; and D/d appears to decrease with increased cable diameter, indicating lesser influence of the bending stresses in thicker cables.

TABLE III.
Smallest Sheave Diameter D for which the Ultimate Tensile Strength of the Cable Loops equals that of the Cable Tested in Direct Tension.

Cable dia. D.mm.	Material	Straight loop Sheave dia. D.mm.	D/d	Crossed loop Sheave dia. D.mm.	D/d
6.3	soft wire	100	16	100	16
10.5	" "	200	19	250*	24*
14.7	" "	250*	17*	300*	20*
18.9	" "	300*	16*	350*	19*
7.5	hard wire	200	27	250*	33*
12.5	" "	250*	20*	300*	24*
17.8	" "	300*	17*	350*	20*

* by extrapolation

For crossed loops the corresponding ratios amount to D/d = 20 with soft wires and D/d = 26 with hard wires. This means that with crossed loops relatively larger minimum sheave diameters are required. As Fig. 6 shows, the minimum sheave size requirements of the cables composed of soft wires increase rapidly when increasing the cable diameter from 6.3 to 10.5 mm. and less rapidly with further cable diameter increases. This feature, it will be noted, is absent in the case of the cables composed of hard wires, where an almost straight line characteristic obtains. The average relationship between cable thickness and minimum sheave diameter is approximated by curve "a" applying to the straight loop arrangement, and curve "b" applying to the crossed loop. The fact that the latter curve lies above curve "a" can be explained by the larger arc of contact peculiar to the crossed loop arrangement.

Fatigue with Cyclically varied Tensile Load.

It was also of interest to investigate the effect of cable diameter upon fatigue strength under pulsating load. A test was carried out on the cables listed in Table IV. with the aid of a Losenhausen direct-stress fatigue testing machine operating at 665 load cycles per minute. The sample pieces of 500 mm. effective length were fixed in grip pots filled with a lead-antimony-tin alloy at 250 deg. C. The tripping device of the machine was adjusted to such a sensitivity that breaking of a few wires brought it into action. Failures mostly occurred at the ends where the cable entered the pot and rarely in the uniformly loaded length. Although the failures took place at points where additional stresses existed, the diagrams can nevertheless be used for evaluating the behaviour of cables under pulsating tensile load.

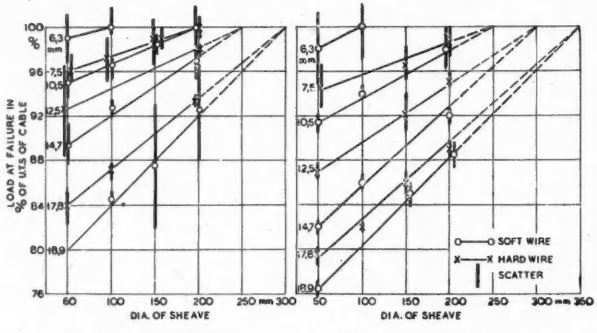

Fig. 4. **Straight cable loop** Fig. 5. **Crossed cable loop.**

Figs. 4 and 5. Ultimate tensile load of cable loops in per cent of U.T.S. in straight-line loading.

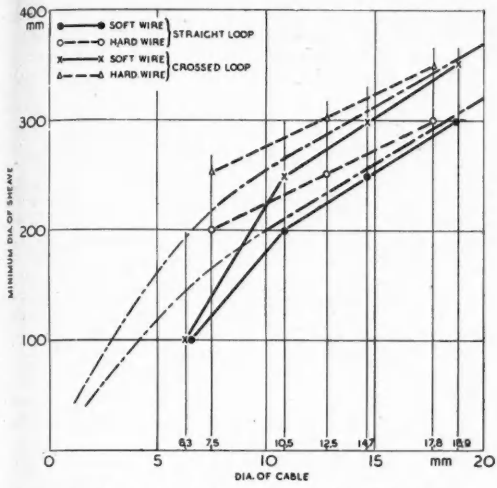

Fig. 6 (left). **Smallest sheave diameter for which the U.T.S of the cable loop equals the U.T.S. in straight-line tension**

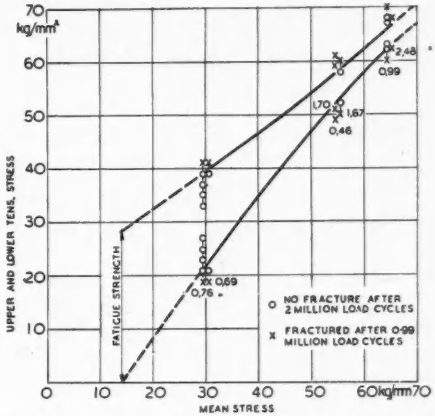

Fig. 7 (above). **Fatigue strength of 10.5 mm. diam. cable No. 1 made of soft wire.**

TABLE IV. **Construction of Cables used for Fatigue Tests.**

Cable No.	Wire	Cable Dia mm.	Core	Number of wires Layer 1	2	3	4	Total	Wire Dia. mm.
I	soft, abt. 90 kg/sq.mm. U.T.S.	10.5	1	6	12	—	—	19	2.1
II		18.9	1	6	12	18	24	61	2.08
III	hard, abt. 170 kg/sq. mm. U.T.S.	17.8	1	6	12	18	—	37	2.5
IV		23.0	1	6	12	18	24	61	2.5

The results obtained with a 10.5 mm. diameter cable No. I composed of soft steel wire of 93 kg. per sq. mm. ult. tensile strength, are shown in Fig. 7, where it is seen that with a stress pulsation between 27 and 33 kg. per sq. mm. (30 kg. per sq. mm. mean stress), 2.01 million load-cycles were carried without failure. When increasing the range of pulsation to 25-35 kg. per sq. mm. (thus retaining a mean stress of 30 kg. per sq. mm.), the cable withstood 2.04 million stress-cycles without failure. The amplitude of stress pulsation was then gradually increased until a wire of the outer layer failed after 0.76 million cycles, the pulsating stress range being 19—44 kg. per sq. mm.

Although it could hardly be expected that with an individual strength of 93 kg. per sq. mm. of the individual wires, the progressively increased stress would create strain hardening, this matter was nevertheless gone into by subjecting sample No. 2 to load pulsations between 21 and 39 kg. per sq. mm. Under this condition, three million load cycles could be carried without fracture; but failure, signified by the breaking of 7 wires of the top layer took place after 0.69 million load cycles between 19—41 kg. per sq. mm. stress. The wire fractures in all cases were confined to the top layer.

Hoisting cables are usually loaded up to 10 per cent of their breaking strength. Therefore, according to diagram Fig. 7, cable No. 1 with a permissible loading of about 8 kg. per sq. mm., should be able to sustain maximum loading of 30 kg. per sq. mm. through 2 million cycles without failure; but such an overload is hardly likely to occur in practice.

In order to give a comparison of the different cables on the basis of cable diameter and of ultimate strength, fatigue test results obtained are combined in Table V. For the cables I. and II., made with soft steel wire, the fatigue strength amounts to 34 and 25 per cent respectively of the ultimate tensile strength of the cable; while for the cables III. and IV., made with hard wire, the respective fatigue strengths are given as 19 and 15 per cent of the ultimate tensile strength. This proves that in both types of cable the fatigue strength is decreased with increased cable diameter.

TABLE V.
Data on Strength of Cables Tested and Wire used in their Manufacture.

Cable No.	CABLE U.T.S. kg/sq.mm.	Assumed Tensile Fatigue strength kg/sq.mm.	% of U.T.S.	Stress pulsation range in Fatigue cycle with mean stress of 20	40	60	80	120 kg/sq.mm.	WIRE U.T.S.	Bending Fatigue strength kg/sq.mm.	Assumed Tensile Fatigue strength kg/sq.mm.
I	81.7	14 ± 14	34	24	14	6	≈1	—	—	—	—
II	88.0	11 ± 11	25	20	16	10	6	—	92.5	± 33	20 ± 20
III	146.0	14 ± 14	19	26	20	14	8	6	172.5	± 40	24 ± 24
IV	152.5	11 ± 11	15	20	15	10	5	9	—	—	—

SAVING AND SUBSTITUTION OF CRITICAL MATERIALS.

(From *La Technique Moderne*, Vol. 35, Nos. 17/18, September, 1943, pp. 133-136.)

AN exhibition was held at the Grand Palais, Paris, on the 19th June, 1943, organised by the Ministry of Industrial Production, at which materials were displayed which have been used, or which it is proposed to use, to replace other materials unobtainable or in short supply owing to the war. Some of these replacements are temporary substitutes only, but others appear likely to hold their place even after the war.

The various stands were organised by the Organising Committees of the various industries, and amongst those of special interest the following may well be described.

BUILDING AND PUBLIC WORKS.

Cement, with barium partly taking the place of calcium. Barytic cement is impervious to X-rays owing to the high atomic weight of barium, thus allowing

of a saving of lead in anti-X-ray revetments in hospital buildings.

Concrete and iron tubes, to replace cast-iron tubes, saving one-half to two-thirds the weight of metal.

Concrete made of stabilised earth, i.e., sand, gravel, with a binder of clay and cement to the amount of 120 to 150 kg. per cubic metre.

Gutters in bakelised wood, replacing zinc. Lighter, easier to handle than fibro-cement.

Pre-stressed reinforced concrete. Reduces weight of steel required and sizes of sections to support given load. Used for railway sleepers, strong but light.

Water-tight tanks for hydrocarbons. The wall of the tank is made in three layers: outside, a wall of reinforced concrete; then a layer of earthenware pierced with channels; and on the inside a thin wall made of granulated concrete, without gravel, which gives a slight porosity owing to very fine veins in it. On the top of the tank is a small pocket of water from which the channels in the earthenware lining are filled. From these channels water infiltrates into the porous concrete of the innermost layer. The tank can then be filled with hydrocarbons, which cannot escape through the porous cement as the veins in it are filled with water under a high capillary tension. The tank is, therefore, hydrocarbon tight, without danger of the water creeping into the tank and mixing with the contents, owing to capillary tension. The usual metal sheeting of the tank is, therefore, replaced by a soaked wall tank with great saving of metal.

MECHANICAL INDUSTRIES.

Moulded plywood impregnated with synthetic resins for aviation and allied industries, e.g., fuselages, gear-cases, etc.

Wooden tubes fretted with steel spirals.

Coppered steel to replace steel for motor-car tubes and pipe-fittings.

Milk containers of sheets galvanised outside and bakelised inside, giving lighter weight than the usual tinned-iron sheets.

Or in almasilium (Al. plus 0.7 per cent magnesium and 1.5 per cent silicon) to replace iron with much lighter weight. (A 10-litre can weighs 3.95 kg. as against 7.5 kg. in iron.)

Welding hard metal surfaces to save steel, e.g., diesel engine valve in Ni. Cr. steel is replaced by mild steel with bearing surfaces of high tungsten steel welded on. In a 37-kg. valve, 5 kg. of Cr, 5.65 kg. Ni., and 1.13 kg. tungsten are saved.

Hard inset teeth for saws.

Pressure pipes of thin sheet, fretted to replace the usual thicker pipes.

Plastic materials (cellulose, resin or polystyrol base) to replace metals, e.g., in water meters.

Zinc, pure or alloyed, in place of bronze for tramway axle boxes; white-metalled steel bearings instead of bronze; bakelised wood or textile products impregnated with synthetic resins for rolling-mill bearings.

Draw hooks kept in service by working up the metal, under heat, into the worn portions.

Artificial rubber replacing packing-leather in brake pistons.

Copper instead of steel in loco-fireboxes.

Aluminium replacing copper in electrical work.

Cellulose skin replacing rubber covering on thin wires.

Synthetic resin tape replacing natural rubber, and acetate rayon replacing silk.

Vulcanised rubber will soon be replaced by artificial rubber or by vinylchloride plastic.

Regeneration of petroleum oils used as insulators.

Copper commutator segments in d.c. motors replaced by steel segments.

Post Office seals on mailbags in aluminium instead of lead.

New system of battery control, allowing elimination of batteries in rural section telephones by a new arrangement of adapters on multiple core cables.

CHEMICAL INDUSTRIES.

Plastic materials, showing astounding advance, chiefly—

1. Bakelite (methane-phenol).
2. Styrol and polystyrol.
3. Phenoplastics (similar to bakelite).
4. Aminiplastics (urea-formal).
5. Cellulose acetate (mixed with vinyl-chloride and vinylacetate).

1 and 2. Electrical accessories.
5. Steering wheel, tools, mallets for aluminium, etc.
5. Clips and fastenings.
4. Knobs, beakers, cups.
5. To replace glass in lamps; tubes and joints in view of pliability, due to vinylchloride. One ton of acetate replaces 6 tons of glass, or 1½ tons of rubber or several tons of tin, copper or steel.

ARTIFICIAL TEXTILES.

Rayon (cellulose acetate silk) already well known; but nylon (hexamethylene-diamine) is now also widely adopted in France. This super-polyamide has properties close to those of animal fibres, with good resistance to alkaline hydrolysis and hydration.

LUBRICANTS AND ARTIFICIAL FUELS.

Oil from schists amounts to nearly 12,000 tons a year; in 1942 this formed 30 per cent of the lubricants distributed by the National Committee.

Anthracene oils (from coal) provide lubricants, antiseptics, etc. Wood products, by decarbonisation of colophane, give 19,000 tons a year.

Synthetic products give 11,160 tons a year; tars and benzoles 21,900 tons per annum; regeneration of used lubricants gives 30,000 tons per annum; biological glycerines give a large amount.

Synthetic processes are—

(*a*) Distillation and carbonisation.
(*b*) Hydrogenation of emulsified solids (Bergius).
(*c*) Hydrogenising synthesis of gaseous products (Fischer-Tropsch or methanal).
(*d*) Hydrolysis of cellulose products by fermentation, giving ethonal and cetonic carburisers. Cellulose from wood, straw, vine-refuse and peat.

GAS PRODUCERS.

Replacement of cotton sheets by glass, rayon, paper, porous china, etc., in filters and so on.

Asbestos joints in hoppers or manholes replaced by metal or glass-wool joints.

Wood cinders from procedures used as manure.

Advantage in beating up carburised mixture before feeding in.

Use of mixture of warm air, steam and water spray.

Panhard generators have now unified 1943 type, which shows a saving in weight of 51 kg., i.e., about 25 per cent over old type C.F.2.

"Lilloise" firebars now made with loose bars to enable replacement of worn bars, 300 gr. each, instead of whole grid weighing 10 kg.

Gohin Tuyeres 1943 all-steel model, saving 3 kg. of copper on old type of all-copper (1941 model hard steel body, copper head).

PURIFIERS.

Panhard new type 28 kg. weight as against 72 kg. old type.

Paper sheets replace cotton in Panhard filters.

Joints in coco-fibre and tar, covered with aluminium foil, replacing asbestos joints.

Imbert coolers (made by Chauson) are to be standardised for every type of producer, to allow of mass production.

THE EFFECTIVENESS OF THE AIRSCREW AS A LANDING BRAKE.

By Dipl. Ing. A. Von der Mühll, Escher Wyss A.G. Zurich. (From *Flugwehr und Technik*, Vol. 5, No. 8, August 1943, pp. 211-217.)

1. INTRODUCTION.

In a previous article* it has been shown by means of an example how the landing run can be cut down by the use of the airscrew as a landing brake.

The present paper gives the designer simultaneously with the theory, a basis for closely estimating the length of run out in a form which has not yet been available in the literature.

2. LANDING WITHOUT BRAKING WITH AIRSCREW.

The landing of an aircraft can be subdivided into four distinct phases: glide, pulling-out from glide, flattening-out, and run out proper (Fig. 1). Thus, the total length required for landing consists of the length of levelling-off d and the length of the run out e.

The landing speed is generally taken as the minimum steady horizontal speed at maximum lift coefficient (with flaps). However, with regard to the danger of stalling, and the aim at a three-point landing, the landing speed V_L is calculated with a lift coefficient $c_a = 0.95\ c_{a\ max}$.

For steady horizontal flight

$$G = A = c_a \cdot \frac{\rho}{2} \cdot V^2 \cdot F \quad .. \quad .. \quad (1)$$

whereby G = Weight of aircraft (kg.)
A = Lift (kg.)
V = Speed (m./sec.)
F = Wing area (m.²)
ρ = Density of air (kg. sec.²/m.⁴)

From eq. (1) $$V = \sqrt[2]{\frac{G/F}{\rho/2 \cdot c_a}} \quad .. \quad .. \quad (2)$$

and the landing speed

$$V_L = \sqrt[2]{\frac{G/F}{\rho/2 \cdot 0.95\ c_{a\ max}}} \quad .. \quad .. \quad (3)$$

3. SIMPLIFIED CALCULATION OF RUN OUT.

The kinetic energy of the aircraft at touch down is spent during the run out by forces of resistance. If the sum of all resistances is P (kg.), the energy equation can be written

$$\int_0^e P\ de = \frac{M}{2} V_L^2 \quad .. \quad .. \quad (4)$$

Herein, e = length of run out (m.),

$$M = \frac{G}{g} = \text{Mass of aircraft (kg./sec.}^2\text{/m.)}.$$

Instead of the rigorous solution, eq. (4), in the present paper mean values will be employed only. For further simplification, the influence of the vicinity of the ground on the plane is neglected. The latter is perhaps by far the greatest neglect inherent in this method. Finally, the coefficient of the ground friction is taken to be independent of landing speed. As all changes are steady in the course of landing, the mean values are obtained by taking arithmetical averages. Eq. (4) thus simplified reads:

$$P_m \cdot e = \frac{M}{2} V_L^2 \quad .. \quad .. \quad (5)$$

The sum of all resistances P_m is composed of the
mean air resistance (drag) W_m
mean wheel friction force R_m and
mean airscrew thrust S_m (see Figs. 2 and 3).

(a) *Landing with Airscrew inactive.*

In the course of the landing the drag W_{ra} at touch down diminishes and reaches the value $W_o = O$ at rest. Therefore, our mean value

$$W_m = \frac{W_{ra} + O}{2} = \frac{W_{ra}}{2} \quad .. \quad .. \quad (6)$$

The friction force between wheels and ground

$$R = \mu\,(G - A) \quad .. \quad .. \quad (7)$$

where μ is the coefficient of ground friction.

As the lift A_{ra} at touch down diminishes to zero at the point of rest, the mean value of R is

$$R_m = \mu\left(\frac{G - A_{ra} + G - O}{2}\right) = \mu\left(G - \frac{A_{ra}}{2}\right) \quad (8)$$

From eq. (1) $G = A_L$, and thus

$$R_m = \mu\left(A_L - \frac{A_{ra}}{2}\right) \quad .. \quad .. \quad (8b)$$

By substituting eq. (6) and (8b) into eq. (5), one obtains

$$\left.\frac{W_{ra}}{2} + \mu\left(A_L - \frac{A_{ra}}{2}\right)\right] e = \frac{M}{2} V_L^2 \quad .. \quad (9)$$

Introducing now for the aircraft mass $M = \frac{G}{g}$

* See "The Airscrew as a Landing Brake" in *The Engineers' Digest*, Vol. IV, No. 8, August 1943, pp. 231-232.

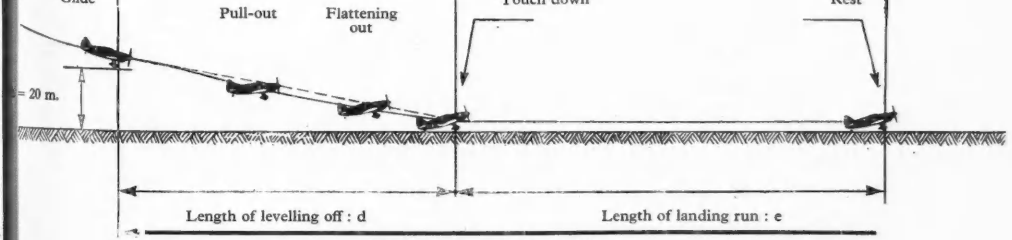

Fig. 1

($g = 9.81$ m./sec.^{2} acceleration due to gravity), and the following non-dimensional coefficients :

Lift coefficient at landing $C_{aL} = \dfrac{A_L}{\rho/2 \cdot V_L^2 \cdot F}$ .. (10a)

Lift coefficient at rolling $C_{ar} = \dfrac{A_{ra}}{\rho/2 \cdot V_L^2 \cdot F}$ .. (10b)

Coefficient of drag at rolling $C_{wr} = \dfrac{W_r}{\rho/2 \cdot V_L^2 \cdot F}$ .. (10c)

eq. (9) becomes

$$e \cdot \frac{1}{2}\frac{\rho}{2} V_L^2 F \left[C_{wr} + \mu (2 C_{aL} - C_{ar}) \right] = \frac{G}{2g} V_L^2 \quad (11)$$

Herefrom the length of the run out

$$e = \frac{G/F}{g \cdot \rho/2 \, [C_{wr} + \mu (2 C_{aL} - C_{ar})]} \quad .. \quad (12)$$

For the orthodox undercarriage with tail wheel another simplification is possible : assuming three-point landing, the angle of incidence is a constant from touch down till coming to rest. Thus, $C_{ar} = C_{aL}$ and $C_{wr} = C_{wL}$. Herewith eq. (12) becomes

$$e = \frac{G/F}{g \, \rho/2 \, . \, (C_{wL} + \mu C_{aL})} \quad .. \quad (13)$$

In eq. (12) the disposition of the undercarriage and the landing technique has a bearing on the bracket expression

$$[C_{wr} + \mu (2 C_{aL} - C_{ar})].$$

It is possible, for instance, that the length of the landing run of a nose-wheel aircraft is smaller than that of an orthodox aircraft with tail wheel if $C_{ar} \ll C_{aL}$. In other words the above bracket expression must then be greater than $(C_{wL} + \mu C_{aL})$.

(b) *Landing run with Airscrew as Brake.*

In first approximation the braking with the airscrew has no influence on the drag of the aircraft, and therefore eq. (6) is still valid. With the airscrew braking, air is blown forward and thus that part of the wing which is in the slipstream does not produce lift. "A" becoming thus smaller, the weight on the wheel (G — A) increases. What percentage of lift is destroyed by the braking airscrew depends on the area of wing lying in the slipstream (Fig. 4). Denoting this area by f, an approximate value for the actually produced lift A_2 can be obtained, assuming that the area (F — f) alone is producing lift.

Thus, $$A_2 = A \frac{F - f}{F} \quad .. \quad .. \quad (14)$$

The load on the wheels is

$$G - A_2 = G - A \frac{F - f}{F} \quad .. \quad .. \quad (15)$$

Under the assumption that the airscrew braking is fully effective from the moment of contacting ground, the friction force becomes

$$R = \mu \left(G - A \frac{F - f}{F} \right) \quad .. \quad .. \quad (16)$$

As the lift at rest is zero the load on the wheels is G, and the mean value of the friction force

$$R_m = \mu \left[\frac{G - A_{ra} \dfrac{F - f}{F} + G}{2} \right] \quad .. \quad (17)$$

Again with eq. (1), $G = A_L$ substituted into eq. (17) we have

$$R_m = \mu \left(A_L - A_{ra} \frac{F - f}{2F} \right) \quad .. \quad .. \quad (18)$$

In addition to the two parameters, Wm and Rm, a third, the negative thrust of the airscrew must now be considered. This is of the value S_{BL} at the moment of touch down, and S_{BO} at rest. (See Fig. 4 of article quoted in the footnote, where the negative thrust for a typical case is plotted against speed).

The mean braking force

$$S_{Bm} = \frac{S_{BL} + S_{BO}}{2} \quad .. \quad .. \quad (19)$$

Substituting eqs. (6), (18) and (19) into the basic equation (5) we obtain

$$\left[\frac{W_{ra}}{2} + \mu \left(A_L - A_{ra} \frac{F - f}{2F} \right) + \frac{S_{BL} + S_{BO}}{2} \right] e = \frac{M}{2} V_L^2 \quad (20)$$

Putting for $M = \dfrac{G}{g}$ and introducing eqs. (10a, b, c) we have

$$\frac{e}{2}\frac{\rho}{2} V_L^2 F \left[C_{wr} + \mu \left(2C_{aL} - C_{ar} \frac{F - f}{F} \right) + \frac{S_{BL} + S_{BO}}{\rho/2 \, . \, V_L^2 F} \right] = \frac{G}{2g} V_L^2 \quad .. \quad (21)$$

Herefrom the length of the run out with the airscrew as brake

$$e = \frac{G/F}{g \, . \, \rho/2 \left[C_{wr} + \mu \left(2C_{aL} - C_{ar} \dfrac{F - f}{F} \right) + \dfrac{S_{BL} + S_{BO}}{\rho/2 \, . \, V_L^2 F} \right]} \quad (22)$$

For the three-point landing of a tail-wheel aircraft $C_{aL} = C_{ar}$ and with C_{wL} for C_{wr} eq. (22) is simplified to

$$e = \frac{G/F}{g \, . \, \rho/2 \left[C_{wL} + \mu C_{aL} \dfrac{F + f}{F} + \dfrac{S_{BL} + S_{BO}}{\rho/2 \, . \, V_L^2 F} \right]} \quad .. \quad (23)$$

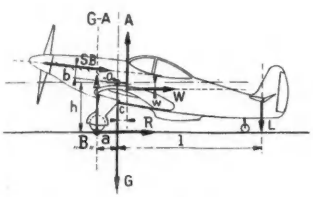

Fig. 2. **Forces at landing.** Tail wheel aircraft).

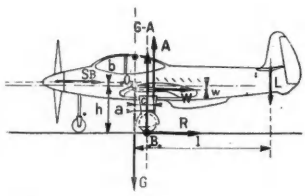

Fig. 3. **Forces at landing.** (Nose wheel aircraft).

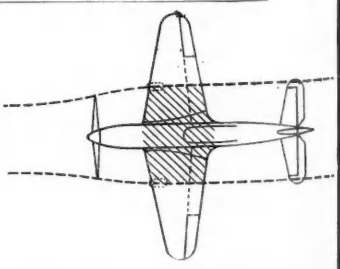

Fig. 4. **The area of wing in the slipstream**

4. THE COEFFICIENT OF FRICTION.

The previous chapter presupposes the knowledge of the coefficient of friction. This embraces the influence of the deformation energy of the ground and of the tyres, the rolling friction of the wheel, the energy of the springing undercarriage, the bearing friction of the wheel axles, and the frictional torque of the wheel brakes. Values of μ are tabulated (Table I), and have been obtained partly from available literature (ZFM, 1927, p. 25 ; Luftwissen, 1941, p. 91 ; NACA.T.R. 583 ; LFF., 1941, p. 70), partly evaluated from measurements on hand of the above simplified formulae.

TABLE I.

	Without brakes		With brakes	
	Min. value	Mean value	Mean value	Max. value
Dry concrete (tail wheel)	0.020	0.030-0.040	0.30	0.40
Dry concrete (nose or tail wheel, air-screw brake) ..	0.020	0.030-0.040	0.40-0.50	Up to 1,000
Dry hard grass (tail wheel)	0.035	0.070-0.10	0.30	0.40
Dry hard grass (nose or tail wheel, air-screw brake) ..	0.035	0.007-0.10	0.40-0.50	Up to 0.60
Wet concrete ..	0.030	0.050	0.30	Up to 0.50
Wet grass	0.060	0.10-0.12	0.20	0.250
Snow or ice covered airfield	0.020	0.010-0.120	0.10	0.150

5. THE DANGER OF NOSING OVER.

With the orthodox tail wheel aircraft there is a danger of nosing over as soon as the moment of wheel friction about " O " (the C.G. of the aircraft) is greater than the tail moment (Fig. 2). From the equilibrium of moments, neglecting the reaction of the tail wheel

$$\mu \leqq \frac{a}{h} + \frac{L \cdot l}{(G-A)\,h} - \frac{A \cdot c}{(G-A)\,h} - \frac{W \cdot w}{(G-A)\,h} \quad .. \quad (24)$$

In the limiting case of rest this expression reduces to

$$\mu \leqq \frac{\mu}{h} \quad .. \quad .. \quad .. \quad (25)$$

This is the ratio of the horizontal and vertical distances from the C.G. of the wheel contact point " B," and its optimum value (low-wing aircraft) can be abt. 0.4. (This limitation is taken into account in Table I).

The negative thrust of the airscrew gives a moment which is opposed to nosing over, unless the axis of thrust lies below the C.G. With airscrew braking eq. (24) can be written

$$\mu \leqq \frac{a}{h} + \frac{L \cdot l}{(G-A)\,h} + \frac{S_B\, b}{(G-A)\,h} - \frac{A \cdot c}{(G-A)\,h} - \frac{W \cdot w}{(G-A)\,h} \quad (26)$$

Towards the end of the landing this expression tends to

$$\mu \leqq \frac{a}{h} + \frac{S_B \cdot b}{G \cdot h} \quad .. \quad .. \quad (27)$$

As long as b is positive (and this is generally the case) μ is here greater than that without airscrew braking.

At rest the negative thrust has a great stabilising effect :

$$S_{BO}\,(b + h) + G \cdot a = P\,(1 + a) \quad .. \quad (28)$$

where P is the reaction of the trail wheel. Eq. (28) is the equilibrium condition about " B," and due to the stabilizing effect there is no danger of nosing over towards the end of the run out, so that the wheel brakes can be more effectively used. With the nose-wheel undercarriage there is no danger of nosing over, be it with or without the airscrew as brake. Instead, one would imagine, after the aircraft has come to rest the negative thrust would cause the aircraft to turn back on to the tail skid. In this case the moment equilibrium about " B " (Fig. 3) enables us to write similarly to eq. (28), and putting the reaction of the nose wheel zero :

$$\frac{S_{BO}}{G} = \frac{a}{b + h} \quad .. \quad .. \quad (29)$$

The ratio $\frac{S_{BO}}{G}$ can be of a maximum value of 0.3.

This ratio is confirmed by the geometry of most of the existing nose wheel designs. It is advantageous to put the airscrew axis in nose wheel designs as low as possible.

6. LANDING WITH EXCESS SPEED.

When landing with a tail wheel type aircraft with excess speed, equation (12) is valid only if the values Cw_r and Ca_r are replaced by mean values

$$Cw_{rm} = \frac{Cw_L + Cw_r}{2} \quad .. \quad .. \quad (30)$$

$$Ca_{rm} = \frac{Ca_L + Ca_r}{2} \quad .. \quad .. \quad (31)$$

(Indices : L = Landing ; r = rolling.)

With nose wheel aircraft eqs. (12) and (22) are valid also for landing with excess speed without modification.

7. CONCLUSION.

The author has shown on hand of examples that the conclusions he reached in a general way in his previous article (see footnote) are fully valid, and that the air-screw brake offers advantages to any type of aircraft. Applied to the orthodox aircraft with tail wheel, advantages can be secured to this type which have been till now attributed to the nose wheel type alone. This appears the more remarkable as the undercarriage of the orthodox type weighs about 40 per cent less than that of the nose wheel type.

In a future article it will be shown that the airscrew described is capable of improving the take-off also. This is of great importance as with the shortened run out the take-off becomes the decisive factor for the necessary dimensions of the airfield.

SELF-CLOSING VALVE FOR PRESSURE GAUGES.

By M. VENOT. (From *Journal des Usines a Gaz*, Vol. 67, No. 8, Aug. 15th, 1943, pp. 91-92).

FREQUENT breakage of compressed gas pressure gauges at the gas compressing stations of the Lyons Gas Company has led on several occasions to the outbreak of fires, since the flame escaping from the gauge made approach to the stop valve of the gauge impossible. In order to eliminate this danger, a special safety device was developed which interrupts automatically the flow of gas to the broken gauge. In this emergency shut-off valve shown in the accompanying drawing, the valve organ consists of a small ball which is pressed down on its seat by the action of the escaping gas, thus stopping the gas flow at once.

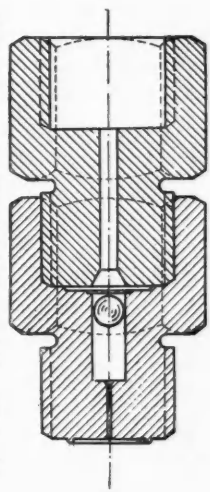

MODERN ISOLATING SWITCHES FOR INDOOR USE.

By H. MANZINGER. (From *E.T.Z., Elektrotechnische Zeitschrift*, Vol. 64, Nos. 1-2, 14th January, 1944, pp. 7-12).

IN high-tension switch-gear installations, breakdowns of isolating switches are often unavoidable and may result in far-reaching plant troubles. Also, as failure of an isolating switch to act as a disconnecting organ may endanger life and safety of personnel, the highest operational reliability of this type of switch is imperative. Another condition necessary in isolating switch design and choice is that its short circuit capacity must not be smaller than that of the circuit breaker served. In the layout of switch-gear, the isolating switches are frequently dimensioned from the aspect of their continuous current-carrying only which constitutes a grave disadvantage. This shortcoming is often due to the fact that isolating switch makers fail to supply any data regarding the short circuit capacity of their product. It may happen, therefore, that isolating switches are installed which are incapable of withstanding the short circuits which may occur. On the other hand, the installation of unnecessarily large isolating switches constitutes a waste of material and money. Isolating switches should be designed on the basis of continuous current-carrying capacity and maximum short circuit capacity, as is the usual practice with circuit breakers.

Insulators and insulating materials used in isolating switch construction must be chosen to provide an adequate operational safety margin in a fairly humid atmosphere. This demand is made in view of the fact that in new construction work, the electrical apparatus may be installed and operated before the plant building is properly dried out. Moreover, even in interiors which are normally dry, a certain dampness may be induced by changeable weather conditions. Bakelised paper type insulators can be made fairly moisture-proof by applying one or several protective coats of varnish, this measure, however, calls for an incommensurate amount of labour in the case of low and medium voltage plant The exclusive use of glazed ceramic insulators for isolating switches is therefore recommended. All required minimum clearances must, of course, be adhered to.

Another important point is that isolating switches should be so dimensioned that they can be accommodated within the width of cell required by the breaker served ; and this applies also to their operating mechanism. The smallest possible spacing between the supporting insulators for the individual phases should be aimed at, because in the frequently used single-floor arrangement of switch-gear for medium voltages, a minimum cell height appears particularly desirable. Generally, fulfilment of these requirements will react favourably upon the material requirements of isolating switch construction.

Three-phase construction of the isolating switch with a grounded operating shaft is to be preferred because of ease and simplicity of operation, and the facility which is afforded for the installation of remote position-indicating devices and ancillary equipment. The terminals of the switch must be suitable for the connection of either aluminium or copper bus bars. Provision must also be made for alternative left-hand or right-hand-side attachment of the operating mechanism to the main shaft of the switch. This requirement calls for an equal overhang of the shaft on both sides of the switch, care being taken to maintain the requisite clearances for the voltage specified. The standardisation of the operating mechanism and its components for the various sizes of a given type of switch will be facilitated by adhering to as few shaft sizes as possible.

The need for providing isolating switches which are difficult of access with additional equipment such as remote position indicators, arresting devices, or compressed air operating mechanisms, often becomes apparent only at an advanced stage of design. Delay in completion of orders to meet such belated supplementary requirements can be avoided by providing for the later installation of auxiliary switch equipment on site. This precaution will also facilitate the delivery of switches from available stock. In order to achieve standardisation of spare parts, post-type insulators of isolating switches must be chosen interchangeable with the supporting insulators used in the bus-bar system in question, and the use of special metal inserts cannot therefore be tolerated.

All switch parts should be dimensioned from the aspect of uniform strength. In the past this matter was often treated with neglect, as an examination of out-of-date designs—still available on the market—has shown. For instance, in a 1000 amp. isolating switch of a certain type, the supporting insulators and the switch frame proved to be designed for a dynamic stress equivalent of 160 kA, whilst the contacts were only suitable for a dynamic stress equivalent of 35 kA. At the same time, the contact parts were dimensioned in thermal respects for carrying 90 kA for one second. The elimination of such incongruities in design will lead to a reduction of material requirements.

Owing to the numbers required and their wide range of application, isolating switches can be manufactured on a mass production scale. Special attention should be paid to this point in the design of the switch components, and wherever possible, forming processes should be preferred to machining operations. Savings in material and labour can also be made by the substitution of drop-forgings for castings.

Considerations of the kind outlined above have recently led to the establishment of a new type of isolating switch for indoor use, covering a range of 1-30 kV and with current-carrying capacities up to 1000 amp. In order to obtain an additional margin of safety, the dynamic strength amperage equivalent of this type is fixed at three times the rated breaking capacity of the corresponding circuit breaker type, while the thermal loading, expressed in terms of maximum amperage, permissible for the duration of one second was made the equivalent of the thermal loading that would result from maintaining rated interrupting amperage of the breaker for a period of three seconds. On this basis the ratings of the various isolating switch sizes of this class were established as follows :

Switch size	Rated Amperage	Insulator type	Short Circuit Max. amperage (dynamic)	Capacity Max. amperage (thermal)
1	200	A	30,000	17,000
2	400	A	60,000	33,000
	600	A	60,000	33,000
3	600	B	60,000	33,000
4	600	B	120,000	66,000
	1000	B	120,000	66,000
5	1000	C	120,000	66,000
6	more than 1000	C	180,000	100,000

Actual manufacture of size No. 1 was not considered, as minimum mechanical strength requirements make it impossible to save a considerable amount of material when compared with size No. 2. Also, the demand for switches of such a low rating is considered too small to warrant their manufacture.

All types were designed on the principle of multi-point contact of the contacting surfaces. By combining this feature with certain other design details affecting

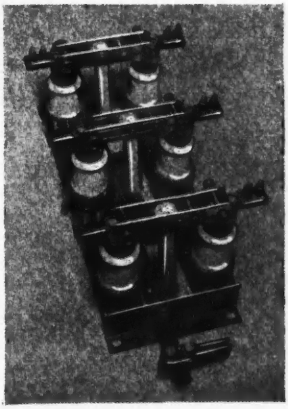

Fig. 1. **Experimental 3-phase isolating switch, size 4, 1000 amp.**

both the movable contact and the fixed contacts, a very high short circuit capacity could be achieved. Investigations conducted on various types of switch-gear have shown that, in the case of a single-point contact with copper as contact material, instantaneous current loadings must not exceed 20-25 kA if weld formation on the contacting pieces is to be avoided. Therefore, to make an isolating switch of 400 amp. rating capable of carrying transient currents of 60 kA, at least two contacting points must exist between the switch blade and the fixed contacts. As tests have shown, this can only be achieved by making the switch blade as thin as possible, so that the contact pressure causes the blade to conform to the contour of the fixed contact surfaces. U-shaped or deliberately stiffened blades must be considered as unsuitable for large short circuit currents, as with them contact is limited to a single point. An experimental switch of size No. 4 is shown in Fig. 1, where it will be seen that each phase is equipped with contacts and blades of different design, in order to afford a comparison of the various contact operating characteristics.

In switches with small clearance between the phases, the electrodynamic forces arising from short circuit currents are countered by the use of a ribbed blade. This also improves the appearance of the switch, as can be seen from Fig. 2 showing an experimental unit of the 400 amp. type. High specific contact pressure is achieved by the use of helical pressure springs which, because of their external arrangement, are not passed

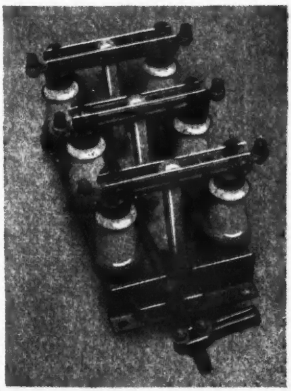

Fig. 2. **Experimental isolating switch, size 2, 400 amp.**

by the electric current (Figs. 1 and 2). This design eliminates the disadvantages of resilient contact pieces in which resiliency was lost by the heating effect of short circuit currents, thus setting a low limit to the latter. Moreover, helical springs as compared to leaf or disc springs possess the advantage of a greater length of travel, thus minimising the influence of manufacturing inaccuracies upon contact pressure.

Certain unsatisfactory properties of bakelised paper insulators have been mentioned before, and the same holds true with regard to the insulated connecting link of the operating mechanism. Connecting links of porcelain with cemented metallic end fixtures cannot be considered satisfactory, particularly as the presence of such metallic parts requires an increase in the clearances between the poles and phases. A novel all-ceramic type of connecting link was therefore developed, as shown in Fig. 3. This new type of ceramic link bears directly upon the respective coupling pins without the interposition of metal parts. A prismatic or oval cross section of the link has proved to be the most suitable shape. Considerable difficulties had to be overcome in narrowing down the manufacturing tolerances of hard porcelain to obtain the required accuracy in dimensions, particularly with regard to the centre to centre distance between the bearings.

Extensive tests were made to ascertain the service reliability of this new type of insulator. Tests extending over a large number of switching cycles conducted

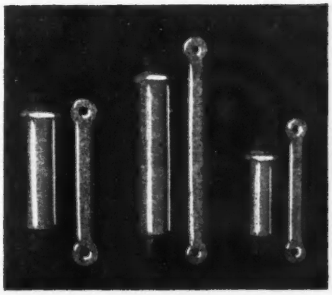

Fig. 3. **Ceramic connecting links (new and old types).**

with several switch types were only concluded with the occurrence of fracture. Likewise, the opening of switches after their exposure to short circuit currents could be successfully carried out without breakage, in spite of the increased forces required to open the seized contacts. A particularly severe test was made by wedging the switch blades in closed position and trying to enforce opening of the switch; but even this rough treatment failed to cause fracture of the connecting link and fractures could be produced only by applying forces large enough to produce failure of the supporting insulators as well. These favourable results are not only due to the choice of steatite as ceramic material, but also to the carefully chosen contour and stress computation of the pieces in which a safety factor of eight to ten based on maximum operational stress was used. Before assembling a switch, each connecting link is subjected to testing at a load 20-25 per cent below fracture load. A typical isolating switch equipped with ceramic connecting rod is shown in Fig. 4, where the salient dimensions for a switch of 600 amp. rating are also given.

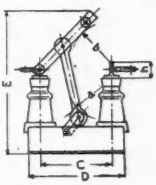

Fig. 4. **New type of isolating switch of 600 amp. rating.**

C = 240 mm. D = 400 mm. E = 530 mm.
h = 60 mm.
a = minimum clearance to earth.
b = minimum clearance for opened switch.

AUTOMATIC MIXER FOR PRODUCER GAS ENGINES.

By PROF. DR. EMIL SCHIMANEK. (From *A.T.Z. Automobiltechnische Zeitschrift*, Vol. 46, Nos. 13-14, July, 1943, pp. 327-335).

TESTS, carried out on producer gas engines, involved the measurement of gas and air supplied to the engine. In order to regulate the pressure in the gas producer and to protect the mixer from contamination by dirt particles, the air, supplied to the producer by means of a roots blower, was measured instead of the gas. A similar blower was also used for the air supply to the mixer. The general arrangement shown in Fig. 1 also reveals a novel fuel control system: the regulating valve is fitted in front of the blowers so that the same pressure is maintained in the generator and in the induction pipe. Calculations indicate that this arrangement is favourable from the view-point of the heating value of the gas, as shown by Fig. 2, where the calorific value is plotted against the quantity of gas generated, for different pressures in the generator. Actual measurements have more than supported this theory, as can be seen from Fig. 3. As a result of this arrangement the heating value of the gas is maintained constant between full load and ¼-full load. The pressure in the system can be adjusted to a suitable value. As an example, it can be regulated to 1 atmos. at full load and hence it becomes slightly less at low loads, or it can be set to 1 atmos. at no load, in which case it increases to about 2.5-3.5 atmos. at full load. In the latter case the engine output and also the filtering efficiency is increased owing to the higher gas pressure. Moreover, the filter dimension can be reduced.

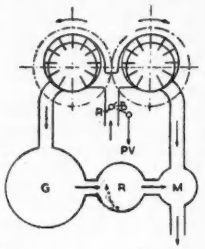

Fig. 1

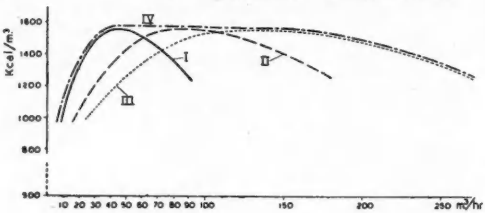

Fig. 2

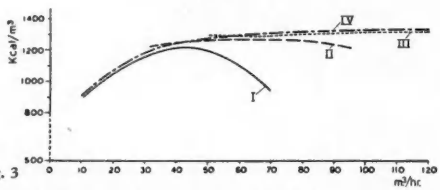

Fig. 3

CHANGE OVER TO THE SIX-STROKE CYCLE.

By adopting a six-stroke cycle the air supply to the generator and the mixer can be controlled by the engine itself. The same principle can be applied also to two-stroke engines. Fig. 4 shows diagrammatically the operation of a six-stroke cycle. During the first two strokes, which precede the normal four strokes, air is taken in by the cylinder (1-2) and forced into the generator (2-3-4). The expansion of the residual air charge in the cylinder takes place during (4-5), while (5-6) is the normal suction stroke. At the beginning of the fourth stroke, gas is forced into the cylinder (6-7) through a valve from the generator where a higher pressure is maintained than in the cylinder corresponding to point (7). The rest of the cycle follows in the usual manner.

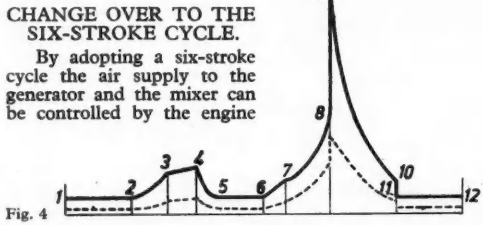

Fig. 4

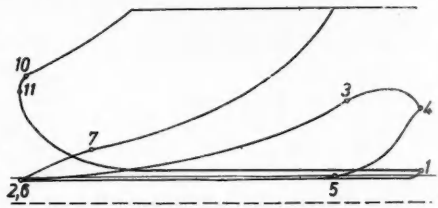

Fig. 5. 1 atmos. = 4.5 mm. (Light spring indicator diagram).

Fig. 6. 1 atmos. = 0.49 mm.

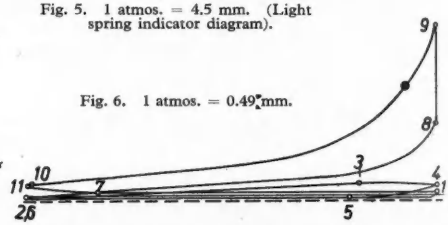

The engine is regulated by a valve in the suction pipe so that at partial load less air is admitted to the engine than at full load. The dotted line in Fig. 4 shows the operation at idling speed. The air intake is only about ¼ of that at full load. Figs. 5 and 6 show indicator diagrams. The principle advantage of the six-stroke cycle is the constancy of air-gas mixture at all loads.

The height of the fire in the hopper was found to remain practically unaltered when the load was changed from full load to no load, and only the intensity of burning decreased. Consequently, after even prolonged running at no load, it took only a few seconds to attain full load again, after opening the throttle.

In two-stroke engines the air is supplied to the mixer by crank case compression, and to the generator, by a blower at a higher pressure than that supplied by the engine. With this system thorough scavenging of the cylinder is ensured which is a further advantage.

CHARCOAL FUEL WITH CONTROLLED WATER INJECTION.

It is well known that the heating value of coal gas is considerably increased if steam is passed over the burning coal. Fig. 7 shows the calorific heating value of generator gas in dependance of steam/burnt coal ratio. In gas producers it is most essential to keep this ratio at the correct value; if the steam supply is insufficient heavy clinker formation might result, while with an excessive steam supply the generator will cool down excessively.

A simple method of regulating the water supply is shown in Fig. 8. A standard carburettor is used, so that the water supply is directly proportional to the

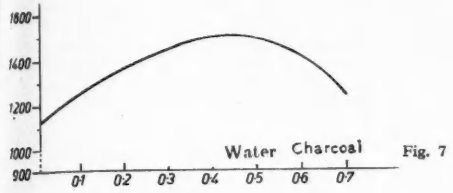

Fig. 7

pressure at the jet level. Since the rate of air flow is proportional to the square root of the pressure, with decreasing air flow the water supply is more rapidly decreased.

Another solution is shown in Fig. 9. The quantity of water passing to the producer is regulated by the valve (8) which in turn is controlled by the diaphragm (5). The water flows past valve (15) where it mixes with air, through the heating coil (18) and into the suction pipe (1) at the inlet (19). The space (3) and also the port (17) are connected to the inlet pressure of the venturi tube (atmospheric in this case). The space (10) between the two diaphragms is connected by means of a tube to the throat of the venturi tube. It can be shown that in this case, too, the quantity of water supplied to the producer is proportional to $\sqrt{Pa-P_1}$.

Fig. 8

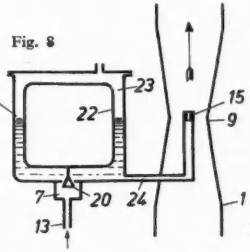

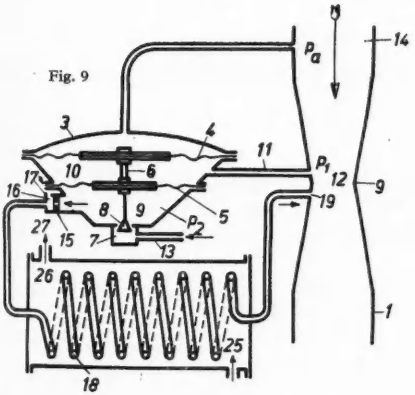

Fig. 9

BURNING WOOD OF 45 PER CENT WATER CONTENT.

If wood of high water content is fired in the generator, serious troubles may arise. Thus, if after prolonged running at full load the engine is suddenly throttled back, the steam generated in the producer provides such a high pressure that no air can enter the hopper. For a short time the engine will draw only steam through the fire zone, with the production of high calorific value water gas, but soon the temperature will drop and the engine eventually stop. To overcome this difficulty provision must be made for condensing the steam. Gas producers were, therefore, developed in which the bottom of the hopper serves as a fire place and the top as a condenser. But in this case both firing and condensing were inefficient. A producer was then developed in which the whole of the hopper area served for heating, and a separate condenser unit is coupled to it by a pipe of large cross sectional area. This design also proved to be a failure owing to the small quantity of steam entering the condenser. Subsequently the design shown in Fig. 10 was adopted, which incorporates an air preheater. The operation of the hopper and condenser are evident from the illustration.

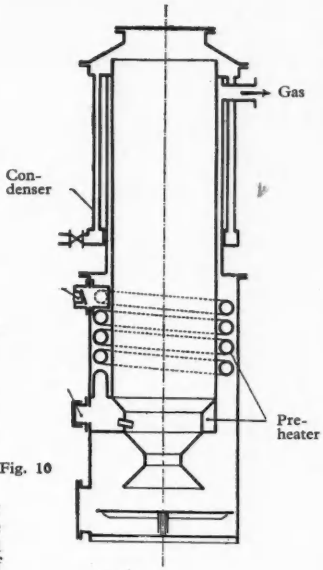

Fig. 10

AUTOMATIC CONTROL OF AIR-GAS MIXTURE.

Two fully automatic air-gas mixtures have been developed in Budapest for use on mobile and stationary engines. The main difference between the two types is due to the fact that vehicles operating at full load consume about 25 times as much air-gas mixture than at no load, while the corresponding ratio for stationary engines is only about 12 to 15:1.

Fig. 11 shows schematically the mixed design for stationary engines. Gas enters through the pipe (26) and air through the pipe (27). (1) and (2) are butterfly valves, the latter being actuated by the diaphragm. The pressures at the sections (38) and (41) respectively act on the two sides of the diaphragm through the channels (40) and (39) so that the air pressure at (41) is kept at the same value as the gas pressure at (38). Thus if the valve (1) is opened the pressure acting on the r.h. side of the diaphragm increases and opens the valve (4) until the two pressures are equalized. In this way the gas-air ratio remains constant at all loads. To provide a richer mixture strength at partial loads, the mixer is slightly modified. On the air side of the diaphragm a

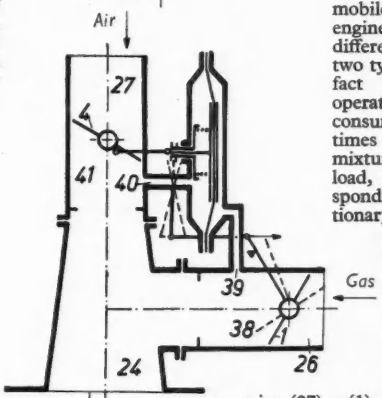

Fig. 11

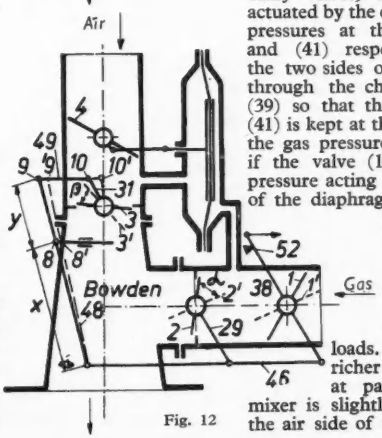

Fig. 12

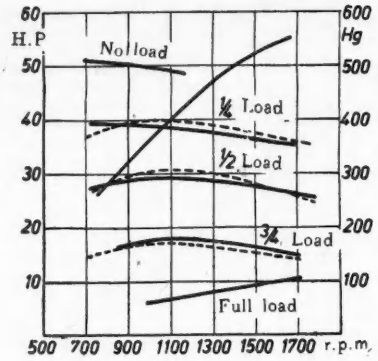

Fig. 13

spring is also provided which does not exert a pressure on the diaphragm when the engine runs at full load but, as the load is gradually decreased so the spring pressure increases and the valve (4) closes. Owing to this additional spring pressure the gas-air ratio increases with decreasing load.

The above mixer does not give satisfactory results with vehicle engines. It was found that the pressure difference (41) and (38) at light loads was insufficient to operate the diaphragm, hence with variations in speed, the gas-air ratio was also altered. If the engine speed went up during light load for some reason, it happened very often that the speed did not fall to normal idling speed but the engine stopped. For this reason two additional valves, (2) and (3), were fitted into the mixer, as shown diagrammatically in Fig. 12. Both these valves are mechanically coupled to valve (1), and hence, owing to the small section of flow the pressure difference acting on the diaphragm was considerably increased. For satisfactory operation, the optimum angular position of valves (2) and (3) must be first determined in the following manner.

Before the mechanical coupling is made up between valves (2), (3) and (1) respectively, the optimum positions 2′ and 3′ at full load, and 2 and 3 at no load, are found by trial and error method. For these positions the lever lengths (49), (48) and (46), and the ratio x/y are determined. Similarly, in the mixer for stationary engines, provision is made to increase the mixture strength slightly at partial loads. For this purpose the fulcrum point (8) of lever (48)-(49) can be shifted to 8′, by pulling a Bowden wire as shown in Fig. 12.

In Fig. 13 the dotted lines indicate the pressure (sub-atmospheric) in the suction pipe for various speeds and loads, at which the fuel is burnt with maximum efficiency. The full lines indicate actual values obtained with the automatic mixer. The difference between the two sets of results is negligible. This mixer was found to give very satisfactory results with diesel-gas engines, that is, where ignition is started by injecting a small amount of liquid fuel into the cylinder.

In Fig. 14 a mixer is shown diagrammatically which is designed to increase the engine output beyond that obtainable with gas fuel only, by also supplying petrol to the engine. The maximum proportion of petrol supplied is limited, so that the producer is kept going under all operating conditions. For this purpose a

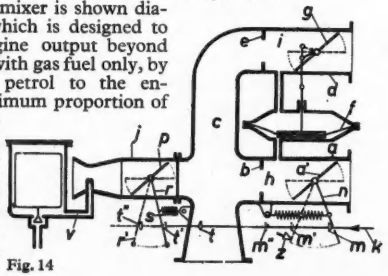

Fig. 14

carburettor, V, is fitted to the mixer, and two valves p and a' are connected to the accelerator pedal. Three critical positions of the pedal are indicated by m, m' and m'' and t, t' and t''. In the positions m and t respectively, gas is only supplied to the engine; at m' or t' the petrol supply is just being opened while the gas throttle corresponding to this position is fully open; at m'' or t' the petrol supply is at maximum. Since both gas and petrol-air mixture are drawn through the same main suction pipe when the valves p and a' are open, part of the air will be drawn through the pipe j and the amount of gas flow correspondingly reduced. In the position m'', the petrol supplied to the engine is about 85 per cent of that with petrol alone, and hence a sufficient gas flow is maintained to keep the fire burning in the producer.

An auxiliary device has also been designed which cuts off automatically the diesel oil supply in diesel-gas engines when the vehicle is driving the engines, e.g., during downward travel on an inclined road. The principle of the device is illustrated in Fig. 15. z-a-c is the suction pipe behind the mixer valve. A small chamber b is connected to the suction pipe through a channel k, and is also open to the atmosphere at the nozzle d. When the engine is driving, the pressure in the chamber is p_1, which is sub-atmospheric and consequently air enters through d. The velocity of the air flow is

Fig. 15

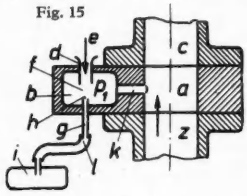

$$c^2 = \frac{2g}{\gamma}(p_a - p_1)$$

where p_a is atmospheric pressure, and γ is the spec. weight of air at the section f. Another channel g, connects the chamber b, to a small, closed vessel i. The pressure at the opening h, is $p_1 + (p_a - p_1)$, i.e., the sum of the static pressure p_1 and that due to the air flow, which is given by $\frac{c^2\gamma}{2g} = p_a - p_1$. Hence the pressure in the vessel is constant at p_a.

When, however, the pressure p_1 falls below a critical value (0.53 p_a) the velocity of air flow through d, does not increase any further and consequently the pressure in the vessel i, drops suddenly under atmospheric. This sudden change in pressure is utilized to actuate an oil cut off mechanism. Fig. 16 shows the results of actual pressure measurements in the vessel i, and confirms that a sudden change of pressure does occur under certain conditions.

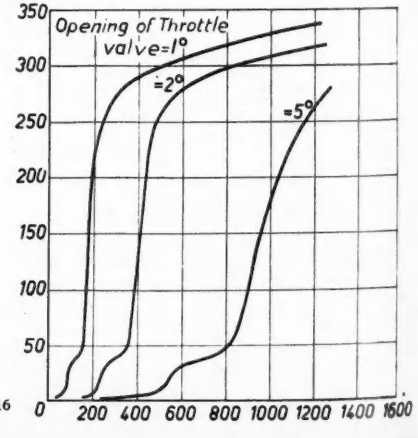

Fig. 16

TECHNICAL NEWS

Announcements in this section include News relating to British Firms, and on Equipment produced by British Manufacturers.

Available literature may be secured by addressing a request to the advertising department of "The Engineers' Digest," or by writing direct to the manufacturer and mentioning "The Engineers' Digest" as a source.

- ✦ NEW EQUIPMENT
- ✦ BOOKS AND CATALOGUES
- ✦ BUSINESS CHANGES
- ✦ PERSONAL
- ✦ NOTES

THE INSTITUTION OF MECHANICAL ENGINEERS
Storey's Gate, St. James's Park, London, S.W.1.

FRIDAY, 19th May at 5.30 p.m. General Meeting "Condensing Locomotives," by Professor G. V. Lomonossoff, Dr.-Ing., M.I.Mech.E., and Cpt. G. Lomonossoff, R.E.M.E.

FRIDAY, 2nd June, at 5.30 p.m. Extra General Meeting in conjunction with the Applied Mechanics Group, "Coupled Engine Torsional and Propeller Flexural Vibrations," by Capt. J. Morris, B.A., followed by informal discussion on Methods of Investigation of Engine Vibration.

THE BRITISH INSTITUTION OF RADIO ENGINEERS
9, Bedford Square, London, W.C.1.

WEDNESDAY, 17th May, at 6.30 p.m. Midland Section Member's Meeting, "Relaxation Oscillators and Trigger Circuits," by Emrys Williams, Ph.D. (Member) at The University of Birmingham, Latin Theatre, Edmund Street, Birmingham.

THE GAUGE AND TOOL MAKERS' ASSOCIATION
Standbrook House, Old Bond Street, London, W.1.

An Export Committee of the Association has recently been formed to assist members in their present export problems and to prepare plans well in advance for a comprehensive post-war development campaign. The constitution of the Export Committee is as follows :— Mr. H. Madeley, Chairman, Brooke Tool Manufacturing Co. Ltd. ; Mr. L. H. Barton, Pitter Gauge and Precision Tool Co. Ltd. ; Mr. J. H. Grant, J. H. Grant & Co. ; Mr. H. H. Harley, Coventry Gauge and Tool Co. Ltd. ; Mr. H. Lainson, Skinners (Redbridge) Ltd. ; and Mr. R. H. Try, Reliance Precision Tools Ltd.

NEW EQUIPMFNT.

VAPOCARB-HUMP METHOD FOR HEAT-TREATMENT OF STEEL.

ANYONE who has a problem involving the heat-treatment of tools, dies or small production parts, may be interested in a 36-page catalogue—"Vapocarb-Hump Method for Heat-Treatment of Steel"—just issued by Leeds & Northrup Company.

The three controls embodied in Vapocarb-Hump furnace equipment—Vapocarb control of atmosphere, automatic control of rate-of-heating and hump control of quench point—are said to provide three important advantages : (1) little or no refinishing ; (2) negligible rejections ; (3) long average tool life. With every phase of the hardening process precisely controlled, and with the tool's heating history recorded visually upon a moving chart, the bare steel—carbon or alloy—is said to leave the furnace with surface free of pits, scale or decarburization ; the heat-treater is able to "ease" work through the critical without the danger of "pushing" and to quench at the exact predetermined point above the hump. Thus, it is claimed, the steel is guarded from abnormal stress and hardening losses due to warpage and breakage are reduced to a minimum.

Copies of the well-illustrated catalogue can be obtained from the Leeds & Northrup Company, 4934 Stenton Avenue, Philadelphia 44, Pennsylvania.

Bi-Way Packing Case Labels. The Bi-Way Label &Printing Co., Temperley, Cheshire, announces a new case label to be used on returnable wooden packing cases and crates. Its design obviates re-labelling, re-tacking, re-addressing, thus speeding up the returning process.

New Soldering and Brazing Machine. The Acru Electric Tool Manufacturing Co. Ltd., 123, Hyde Road, Ardwick, Manchester, 12, has marketed a portable electric soldering and brazing machine which, it is claimed, has the following advantages over soldering irons :—(1) No necessity for cleaning the bits ; (2) Instantly replaceable carbon rods which are cheaper than copper bits ; (3) Machine always ready for use ; (4) Higher thermal efficiency ; (5) No heating elements ; (6) Economic current consumption ; (7) Heaviest as well as finest gauges can be soldered ; and (8) No danger from electric shocks.

Change of Address : The new address of Fusarc Ltd., Letchworth, Herts, will be as from the 12th April :—Fusarc Ltd., Team Valley, Gateshead-on-Tyne, 11. Telephone : Low Fell 75296-7.

HEAT TREATMENT SPECIALISTS

ON APPROVED LIST OF AIR MINISTRY AND ADMIRALTY

- Case Hardening and straightening up to 8 ft. long.
- Hardening all Classes of Sub. and High Speed Steel Tools, Bakelite Moulds and Press Tools.
- Hardening by the Shorter Process.
- Cyanide Hardening, Capacity 3 tons per week
- Springs : Any size, shape or quantity.
- Aluminium Alloys Heat Treated to A.I.D. Specifications.
- Heat Treatment of Alloy Steels up to 10 ft long
- Heat Treatment of Meehanite Castings, etc.
- Crack detecting on production lines.
- Chemical Rustproofing (different colours) to A.I.D. and other Specifications.

THE EXPERT TOOL & CASE HARDENING CO. LTD.
(Est. 1918)
GARTH ROAD, LOWER MORDEN, SURREY.
Telephone : Derwent 3861-2

Bristol for Engineering—
BRISTOL FAMOUS FOR :—
Mechanical, Electrical, Constructional, Aeronautical and Marine Engineering.
Consult the BRISTOL ENGINEERING MANUFACTURERS' ASSOCIATION, 104, FILTON AVENUE, BRISTOL, 7

PERSONAL.

Mr. Raymond Berry has been appointed Chairman and Managing Director of Berry's Electric Ltd.

Mr. J. T. Brockhouse, O.B.E., J.P., Chairman and Managing Director of J. Brockhouse & Co. Ltd., died suddenly on the 20th April at a Meeting of the S.M.M.T.

Sir Summers Hunter has been elected President of the North-East Coast Institution of Engineers and Shipbuilders.

Mr. F. O. John, of Cammell Laird & Co. Ltd., has been elected President of the Liverpool Engineering Society.

Mr. L. S. Kinnear has been elected Director of the British Oxygen Co. Ltd.

Mr. W. P. Lilwall has been elected President of the Incorporated Municipal Electrical Association.

Mr. A. C. Macdiarmid, Chairman and Managing Director of Stewarts and Lloyds Ltd., has been elected President of the British Iron and Steel Federation.

Mr. A. McArthur, of 360, Farm Street, Hockley, Birmingham, has been appointed Local Director of the Electric Furnace Company Ltd.

Mr. Harold F. Massey has been elected Chairman, and **Mr. C. E. P. Hayton** and **Mr. Keppel F. Massey** have been appointed joint Managing Directors of B. and S. Massey Ltd.

Sir David Milne-Watson has been elected Governor of the Gas Light and Coke Company. **Mr. Henry Woodall** and **Sir Harold Hartley** have been elected Deputy Governors.

Sir George Nelson, Chairman and Managing Director of the English Electric Company Ltd., has been elected President of the Federation of British Industries for his second year of office.

Mr. E. D. O'Brien, Director of the Press Division of the British Council since its inception in 1938, has resigned to take up an important executive post with Rootes Securities Ltd.

Mr. J. L. Rowbotham has been appointed Director of Switchgear and Cowans Ltd.

Mr. John Shearman, M.I.Mech. E., Road Motor Engineer of the L.M.S.R., has been elected President of the Institution of Automobile Engineers. **Mr. W. W. Constantine, Capt. G. T. Smith-Clarke,** and **Mr. Frank G. Woolard** have been elected Vice-Presidents.

Mr. H. N. Sporborg, Chairman of the British Thomson-Houston Co. Ltd., has been elected Director of the Lancashire Electric Light and Power Co. Ltd.

Mr. I. A. R. Stedeford has been appointed Chairman of Tube Investments Ltd.

Mr. R. Alan Thwaites, M.Inst.C.E., M.I.E.E., has been appointed Chief Engineer and Manager to the Manchester Corporation Electricity Department.

Mr. F. S. Whalley has been appointed Chairman of Robert Stephenson and Hawthorns Ltd.

BRITISH STANDARDS.

(Copies of British Standards may be obtained from the British Standards Institution, 28, Victoria Street, London, S.W.1).

BRITISH STANDARD FOR BUTT-WELDED BLANKS FOR CUTTING TOOLS (B.S.1119:1943).

BUTT-WELDED blanks have been used in the tool manufacturing industry for many years and experience has shown that tools produced from such blanks are equal in performance to those produced from high speed steel, provided certain precautions are taken in the design, and that an appropriate method of heat treatment is used.

The necessity for conserving high speed steel has led the Ministry of Supply to co-operate with the tool manufacturers and the British Standards Institution in the preparation of a war emergency British Standard which establishes the dimensions of such blanks, comprising a high speed steel portion butt welded to a medium carbon steel shank, for the manufacture of shank type cutting tools such as lathe and planer tools, twist drills, reamers, milling cutters and machine nut taps.

The standard describes a recommended heat treatment and also includes an appendix giving the weight of high speed steel for each size of blank. Price 2/-.

STANDARD CODE FOR THE USE OF CATHODE-RAY TUBES, B.S. 1147.

WITH a view to giving guidance to the designers of radio and other equipment containing cathode-ray tubes as to how to obtain the optimum life and performance, some instructions have been drawn up by a committee of British cathode-ray tube manufacturers working in collaboration with the British Radio Valve Manufacterers' Association.

The importance of consulting the cathode-ray tube specifications before undertaking the design of equipment is emphasised, and collaboration with the cathode-ray tube makers is advised in cases where exceptional needs arise, or where the tube is to be put to a use which does not appear to be covered by the tube specification. Sections of the code then deal with the tube dimensions ratings, heater voltage regulation, mounting, ventilation, heater/cathode insulation, grid circuits, plate circuits, focussing, characteristic limits and general conditions. Price 6d.

B.S.156.—REVISED STANDARD FOR ENAMELLED WIRES

A NEW grade of enamelled wire has been introduced into the specification B.S. 156. This new grade has a heavier coating of enamel, and the original grade and the new grade are now designated "normal covering" and "thick covering" respectively, the latter being sometimes referred to in the trade as "double enamelled wire."

The specification defines the quality of the copper, the thicknesses of enamel, and the limits of resistance. Electrical and chemical tests are included.

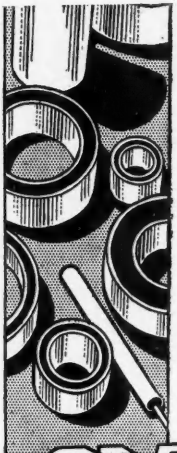

Eliminate Lubrication

Stop Vibration
Reduce Noise
Transmit Power
Prolong Life
Low Cost
Unaffected by dirt, dust, grit or water

Our technical staff will be pleased to assist at any time in putting forward suggestions where CLAYFLEX BEARINGS could be applied.

The rubber and metal are one unit after being Mechanically Bonded.

CLAYFLEX
FLEXIBLE BEARINGS

CLAYFLEX LTD.
TIDDINGTON RD. STRATFORD-ON-AVON
PHONE: STRATFORD-ON-AVON 3296/7
GRAMS: CLAYFLEX, STRATFORD-ON-AVON

FROM NATIONAL SERVICE TO SALES SERVICE

TOOL UP WITH CHROME ALLOY BRITOOL SOCKET WRENCHES

YOU CHANGE OVER WITH THE SAME KIT
Britool are, year in year out, the Tools for your Trade. A life-long investment in efficiency and service. **Service Panels, Interchangeable Sockets, Plugs, Wrenches, Universal Joints, Individual Wrenches, etc. 2,500 designs.**

BRITOOL WORKS
BUSHBURY
WOLVERHAMPTON
ENGLAND
Telephone: 31281
Telegrams: "Jenbro"

JENKS BROS. LIMITED

NORTHERN OFFICE
VICTORIA CHAMBERS
SOUTH PARADE
LEEDS
Telephone: 26776
Telegrams: "Chamfer"